1-1-2017

3D network of cellulose-based energy storage devices and related emerging applications

Saikat Dutta
National Taiwan University

Jeonghun Kim
University of Wollongong, jhkim@uow.edu.au

Yusuke Ide
National Institute for Materials Science, Japan

Jung Ho Kim
University of Wollongong, jhk@uow.edu.au

Md. Shahriar Al Hossain
University of Wollongong, National Institute for Materials Science, Japan, shahriar@uow.edu.au

See next page for additional authors

3D network of cellulose-based energy storage devices and related emerging applications

Abstract

There has recently been a major thrust toward advanced research in the area of hierarchical carbon nanostructured electrodes derived from cellulosic resources, such as cellulose nanofibers (CNFs), which are accessible from natural cellulose and bacterial cellulose (BC). This research is providing a firm scientific basis for recognizing the inherent mechanical and electrochemical properties of those composite carbon materials that are suitable for carbon-electrode applications, where they represent obvious alternatives to replace the current monopoly of carbon materials (carbon nanotubes, reduced graphene oxide, and their derivatives). Significant promising developments in this area are strengthened by the one dimensional (1D) nanostructures and excellent hydrophobicity of the CNFs, the interconnected pore networks of carbon aerogels, and the biodegradable and flexible nature of cellulose paper and graphenic fibers. Outstanding electrode materials with different dimensions (1D, 3D) are derivable by the strategic choice of cellulose sources. This development requires special attention in terms of understanding the significant impact of the cellulose morphology on the final electrochemical performance. This review article attempts to emphasize the role of the different structural forms and corresponding composites derived from different forms of cellulose, including bacterial cellulose and its varied 3D nanostructures. This article strongly highlights that cellulose deserves special attention as an extremely abundant and extensively recyclable material that can serve as a source of components for electronic and energy devices. Along with emphasizing current trends in electrochemical device components from cellulose, we address a few emerging areas that may lead in future such as enzyme immobilization, flexible electronics, modelling of cellulosic microfibrils. Finally, we have discussed some of the important future prospects for cellulose as source of materials for future.

Disciplines

Engineering | Physical Sciences and Mathematics

Publication Details

Dutta, S., Kim, J., Ide, Y., Kim, J., Hossain, M. A., Bando, Y., Yamauchi, Y. & Wu, K. C-W. (2017). 3D network of cellulose-based energy storage devices and related emerging applications. Materials Horizons, 4 (4), 522-545.

Authors

Saikat Dutta, Jeonghun Kim, Yusuke Ide, Jung Ho Kim, Md. Shahriar Al Hossain, Yoshio Bando, Yusuke Yamauchi, and Kevin C.-W Wu

Volume 4 | Number 4 | July 2017 | Pages 513–710

Materials Horizons

rsc.li/materials-horizons

ISSN 2051-6347

ROYAL SOCIETY OF CHEMISTRY

REVIEW ARTICLE
Yusuke Yamauchi, Kevin C.-W. Wu *et al.*
3D network of cellulose-based energy storage devices and related emerging applications

Materials Horizons

REVIEW

View Article Online
View Journal | View Issue

Cite this: *Mater. Horiz.*, 2017, 4, 522

3D network of cellulose-based energy storage devices and related emerging applications

Saikat Dutta,†[a] Jeonghun Kim,[b] Yusuke Ide,[c] Jung Ho Kim,[b] Md. Shahriar A. Hossain,[bc] Yoshio Bando,[c] Yusuke Yamauchi*[bc] and Kevin C.-W. Wu*[a]

Received 9th November 2016,
Accepted 13th February 2017

DOI: 10.1039/c6mh00500d

rsc.li/materials-horizons

There has recently been a major thrust toward advanced research in the area of hierarchical carbon nanostructured electrodes derived from cellulosic resources, such as cellulose nanofibers (CNFs), which are accessible from natural cellulose and bacterial cellulose (BC). This research is providing a firm scientific basis for recognizing the inherent mechanical and electrochemical properties of those composite carbon materials that are suitable for carbon-electrode applications, where they represent obvious alternatives to replace the current monopoly of carbon materials (carbon nanotubes, reduced graphene oxide, and their derivatives). Significant promising developments in this area are strengthened by the one dimensional (1D) nanostructures and excellent hydrophobicity of the CNFs, the interconnected pore networks of carbon aerogels, and the biodegradable and flexible nature of cellulose paper and graphenic fibers. Outstanding electrode materials with different dimensions (1D, 3D) are derivable by the strategic choice of cellulose sources. This development requires special attention in terms of understanding the significant impact of the cellulose morphology on the final electrochemical performance. This review article attempts to emphasize the role of the different structural forms and corresponding composites derived from different forms of cellulose, including bacterial cellulose and its varied 3D nanostructures. This article strongly highlights that cellulose deserves special attention as an extremely abundant and extensively recyclable material that can serve as a source of components for electronic and energy devices. Along with emphasizing current trends in electrochemical device components from cellulose, we address a few emerging areas that may lead in future such as enzyme immobilization, flexible electronics, modelling of cellulosic microfibrils. Finally, we have discussed some of the important future prospects for cellulose as source of materials for future.

1. Introduction

The current thrust for fabricating high-performance three-dimensional (3D) carbon nanomaterials from lignocellulosic biomass (*e.g.*, cellulose and lignin) provides scope for the next level of development of materials for flexible energy storage and supply devices. The large global reserves of renewable cellulose together with its known potential as a platform for deriving functional materials means that it is already widely used, albeit primarily in low-tech applications to date, such as information storage and packaging applications. Recently, however, there has been emerging interest in utilizing these materials in advanced technologies as well; for instance, as functional components (*e.g.* energy storage).[1–3] Remarkably, cellulosic material with an ordered mesoporous structure is highly favorable for the development of a new range of applications.[4] Consequently, engineered porous carbon materials, obtained by the pyrolysis of biomass materials (agricultural and forestry residues) in an oxygen-limited environment, are also playing an increasingly important role in the ongoing development of a more sustainable economy and for fixing carbon for environmental protection.[5]

Over the past decade, increasing attention and efforts have been focused on the development of alternative energy sources and energy storage devices to alleviate the impacts of climate change and fossil fuel depletion. The development of practical energy storage devices for carrying and delivering the desired energy has turned into a priority to support the efforts to produce renewable energy from the sun and other renewable sources.[6] Batteries and supercapacitors offer much higher

[a] *Department of Chemical Engineering, National Taiwan University, No. 1, Sec. 4, Roosevelt Road, Taipei 10617, Taiwan*
[b] *Australian Institute for Innovative Materials (AIIM), University of Wollongong, Squires Way, North Wollongong, NSW 2500, Australia. E-mail: yusuke@uow.edu.au*
[c] *International Center for Materials Nanoarchitectonics (MANA), National Institute for Materials Science (NIMS), 1-1 Namiki, Tsukuba, Ibaraki 305-0044, Japan*
† Current address: Catalysis Center for Energy Innovation (US DOE EFRC), University of Delaware, Newark, Delaware 19716, USA.

cycling stability and power density, but suffer from low energy density.[7] Furthermore, another trend is for flexible and wearable electronics, which are gaining significant importance due to their suitability for wide integration and their portability, with the added advantage of that they can undergo structural transformation to form supercapacitors, batteries, and flexible solar cells.[8–10] Among the current strategies for energy storage in supercapacitors, high power and good cyclability are the two most desirable features. There are two different ways to store charge in a supercapacitor, *via*: a non-Faradaic double-layer electrostatic charging process or a Faradaic surface redox process. On the other hand, the lithium-ion battery (LIB) has also received widespread attention for large-scale power sources and energy storage devices, owing to its high power, high energy density, and long cycle life. There is an increasing demand for key LIB materials, especially separators, which serve the crucial functions of physically separating the anode and cathode while allowing the free flow of lithium ions.[11,12] It has been recognized that the microporous structure and thermal dimensional stability of separators considerably affect the battery performance. Given the overwhelmingly growing demand for energy storage devices with high performance for portable electronic applications, lightweight, high power density, durable, and low-cost energy storage devices are the major targets. To meet the increasing energy demands for next-generation supercapacitors and separators, a substantial increase in energy density without sacrificing the power density and cycle life is a major challenge that still needs to be addressed.[13,14]

Cellulose, being one of the most abundant renewable biopolymeric materials, is already widely used in our daily lives. But recent applications of cellulose in the fields of electronics, biomaterials, and pharmaceuticals suggest that the structure and properties of cellulose can promote it beyond the existing range of use in conventional areas.[15–17] Cellulose is the main component of the plant cell wall, with the special features of passing nutrients and maintaining the cell shape through tensile strength (Fig. 1(a)). Native cellulose fibers function like a cell wall, and can take up electrolytes from a bulk electrolyte bath. The electrolytes, such as nutrients, are then transported *via* the pores through a matrix of cellulose fibers, and thus the mesoporous channels inside the fibers act as extra ion-diffusion pathways for charge/discharge processes. This mesoporous structure of cellulose fibers has previously been developed as a nanoreactor for metal nanoparticles (<10 nm) generation[18] and for the growth of zeolites (from wood tissues) (Fig. 1(b)).[19] When using cellulose papers as the source of cellulose fibers (11 m width) with a rough surface and porous network (30–70 nm pore size) (Fig. 1(c)), nanopores can be used as a host for guest molecules, which may then penetrate into the inner space.[18]

Cellulose nanocrystals (CNCs), cellulose microfibrils (CNFs), and bacterial cellulose (BC) are the most commonly used forms of nanocellulose.[20] The most promising aspect of these is that these forms of cellulose offer enormous potential as alternatives to synthetic polymers and stand out in terms of their material properties, which include high strength, low density, a large aspect ratio, and biocompatibility.[21] High-temperature and hydrothermal carbonization to obtain carbonaceous materials from cellulose is the most common way to build conductive carbon structures.[22,23] The degree of graphitization can be improved at higher carbonization temperatures to enhance the ordering of the graphene stacks, although such a high temperature process involving energy consumption does not offer a long-term promising solution to obtaining high-performance cellulose-based materials.

For mimicking well-defined materials in nature and for utilizing natural resources in a sustainable way, the design of functional materials using renewable sources has experienced exceptional growth.[24–26] Wood- and cellulose-based materials have been extensively brought into focus in order to build novel materials for replacing conventional materials that experience substantial challenges in being utilized in energy storage device applications. The unique properties of cellulose nanofibers (CNFs), such as high strength and high length-to-diameter ratio, allow for the preparation of multifunctional materials, such as nanopaper, porous aerogels, and thin films.[27,28] Nevertheless, certain limitations, such as their hydrophilicity and weak wet stability in liquid media, need to be overcome to extend their practical applications.

Physical pretreatment through the mechanical fibrillation of woody biomass is one promising avenue to remove the barrier of needing to gain access to the cellulosic components. Mechanical size reduction to the level of fibers or fiber bundles, such as those in wood pulp production, is also essential. Due to the complexity of the lignocellulosic system, most studies tend to measure the overall production of sugars, and thus, the produced feedstock, such as nanofibrous materials like lignocellulose nanofibrils (LCNFs) produced from wood fibers,[29] typically still contains lignin, hemicellulose, and other biopolymers.

Bacterial cellulose (BC) is an ecofriendly biopolymer produced by various microorganisms (*Acetobactor xylinum*, *Pseudomonas*), and it consists of ribbon-shaped ultrafine nanofibers with widths less than 100 nm.[30,31] The recent development of BC is based on the combination of conducting polymers (polyaniline, polypyrrole) with the BC nanofibers to create fully renewable, biodegradable, and electrically conductive composite materials. When using such materials as supercapacitor electrodes, a high mass-specific capacitance can be achieved. Consequently, BC-based materials exhibit a huge potential as flexible supercapacitor electrodes as hydrophilic BC paper can enhance the contact between the electrodes and aqueous electrolytes, thus providing diffusion channels for electrolyte ions[32] In addition to supercapacitor electrodes, BC has also been found to be suitable for macroscopic-scale carbon-nanofiber aerogels[32] and transparent composites[33] owing to an interconnected nanowire structure in the BC. Cellulose has the unique feature of gathering polymer chains into nanofibrils (so-called CNFs), and applied pressure homogenization can be used for extraction of the nanofibrils from fibers. These fibrils possess a high aspect ratio and are thus more beneficial for the reinforcing phase in a composite. However, it is essential to overcome the aggregation of fibrils by modifying the cellulose functional groups. Superior mechanical strength, the high elastic modulus of a single cellulose fibril, and the ability to form paper sheets with high porosity contribute to creating strong permeable electrolytes based on CNFs.

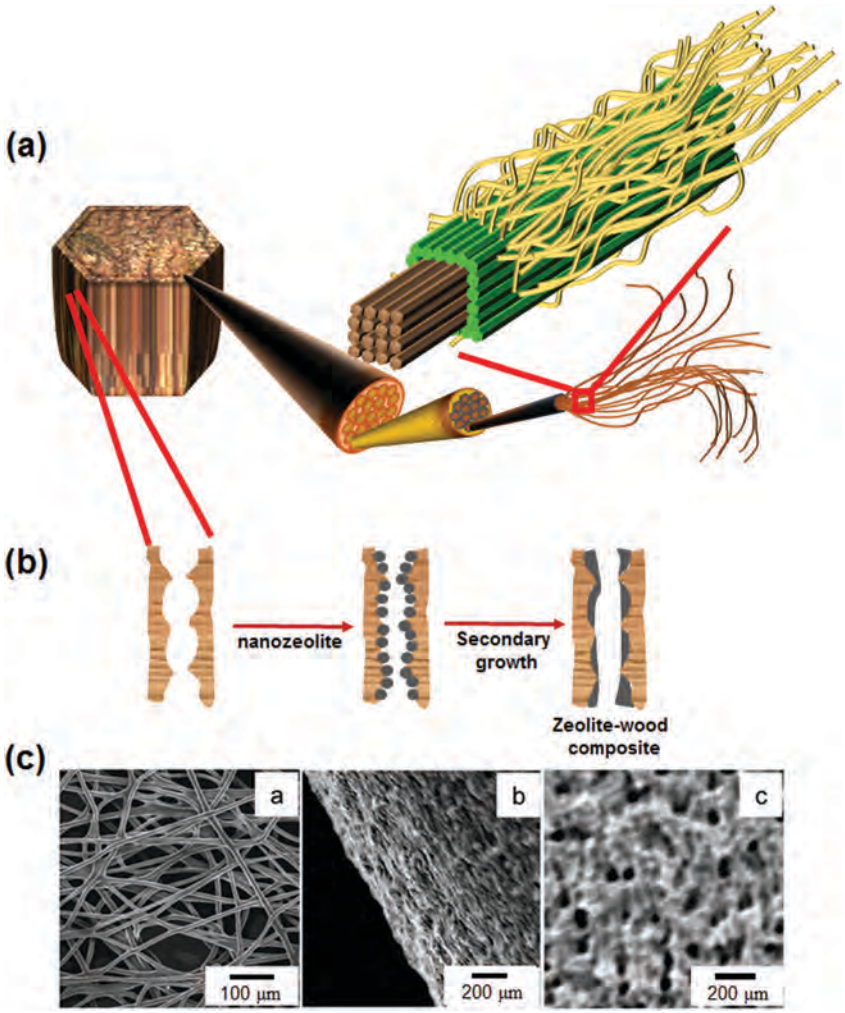

Fig. 1 (a) Mesoporous cellulose with diffusion channels for facilitating the charge–discharge process, (b) cellulose fiber exploited for the growth of zeolites, and (c) from left to right, field-emission-scanning electron microscopy (FE-SEM) images of cellulose paper texture, the edge, and the surface of a single cellulose fiber used for the growth of metal nanoparticles (Ag, Au, Pt, Pd) (reproduced from ref. 18, copyright American Chemical Society, 2003).

In recent years, significant research has been carried out on flexible supercapacitor electrodes derived from cellulosic materials, with special attention paid to recyclable cellulose-based electrodes.[34] Understanding the key role of cellulose in improving the specific capacitance and cycling stability of flexible charge storage devices are one of the major tasks to be completed. Undoubtedly, in the coming decades, flexible devices will include integrated advanced electrical and optical functions, and it is considered that electrodes based on cellulose-derived materials and charge storage applications utilizing such materials will play a role in the further developments. Current trends in deriving aerogels and graphenic fibers are other certain areas in which cellulose-based electrode materials hold long-term promise, and thus we address these inspiring topics in this article.

2. Structural forms of cellulose

Supercapacitors, electrochemical capacitors, and other energy storage devices are the ideal candidates for filling the gaps between conventional devices and devices utilizing components obtained from renewable materials. Cellulose, a major constituent of biomass, can be extracted from waste paper and then utilized for bio-composites for application in energy storage applications. Even though pure cellulose is a non-electroactive material, it is applied in electrochemical energy storage in its different forms. Cellulose fiber has huge possibilities as it is able to adapt its physical and chemical properties according to the requirements of the energy storage application. Owing to its film-forming ability and fibrous nature, cellulose fibers can enhance the mechanical stability of cellulose-based composites. Thus, it is essential to account for the structural features of various forms of cellulose.

2.1. Cellulose nanofibrils

Cellulose nanofibrils (CNFs) are natural cellulose-based nanomaterials and are drawing intensive attention in nanomanufacturing owing to their great abundance, low cost, and firm biocompatibility.[35] Composed of elementary cellulose fibrils directly extracted from natural plant sources, they exhibit comparable

mechanical properties to other generally used materials, such as carbon fibers and glass fibers, along with great adsorbability of both hydrophilic and hydrophobic materials.[36] It is the repeating units of the cellulose polymer chains that are gathered into nanofibrils, *i.e.*, CNFs aggregated into macroscopic fibers obtained from pulp from both plant (Fig. 2(a)) and bacterial cellulose (Fig. 2(b)).[37] In order to extract the fibrils from fibers, pressure is applied in a homogenizing process to enable the fibrils to be collected.[38] Generally, the nanofibrils of cellulose feature a high aspect ratio, which in turn makes them suitable for application as a reinforcing phase in a composite.

Since aggregation is a significant problem with CNFs due to their large surface area compared to their volume, to reduce aggregation, additional oxo-groups (*e.g.*, carboxylate) on the surfaces of the fibers are desirable. This increases the charge density on the surface, while decreasing the flocculation and the tendency toward clogging. Among the outstanding properties of CNFs are: (1) superior mechanical strength (elastic modulus of a single cellulose nanofibril: ~140 GPa), (2) strong enough to form paper sheets with high porosity, and (3) more porosity and ductility, which can be induced by employing solvent exchange procedures using low polarity solvents. The nanodimensions of the structural elements result in a high surface area and, hence, lead powerful interactions of these cellulose fibrils with their surrounding species, such as water, and organic and polymeric compounds. Microfibrils obtained from wood and their applications in nanocomposites, in the preparation of nanocrystalline cellulose, and in the biofabrication of bacterial nanocellulose have promoted applications involving the nanofibrils of cellulose to a new level. Functionalized porous CNFs in a structural composite electrolyte can act as a reinforcing phase in a composite with a polymer matrix that also features ionic conductivity. Post-functionalization of the fibril surface can enhance the interfacial strength in the final composite electrolyte. High-porosity, three-dimensional (3D) nanostructures, for example, branched nanowire architectures (3D NWs) and nanofiber networks, offer an extremely large surface area, superior charge transport features, and long optical paths for efficient light absorption. Thus, 3D nanostructures, especially nanowire (NW) architectures, are the current focus of a tremendous surge of interest in photoelectrochemical devices, as demonstrated by the growth of interest in the TiO_2 NW electrode using Si NW arrays as a backbone (Fig. 2(c)).[39] Thus, 3D nanostructures obtained from CNFs[40] are already being implemented in electrode design, and might have a strong impact on the future design of energy storage devices.

2.2. Bacterial cellulose

The unique structure of bacterial cellulose (BC) exhibits some interesting properties, which shows us that many useful substances are being left unutilized in nature and their underexplored advanced features are not being fully realized. For example, electrically conducting materials capable of substantial elastic stretching and bending are key features that researchers would like to discover in materials that are resourced from biorenewables.[41,42] Among the materials studied so far for various applications that have reached the level of practical use, such as for acoustic diaphragms, BC has been found to offer two essential properties, *i.e.*, high sonic velocity and low dynamic loss.[43] BC has a specific ultrafine network structure and many notable properties, such as sufficient porosity, high tensile strength, high water retention capability, and excellent biodegradability. To date, BC has been utilized as a constituent of 3D hybrid carbon nanomaterials, paper, biosensors, optically transparent films, and flexible optoelectronic devices. A few of the major features that BC is capable of offering in materials derived from it are: (1) transparency, (2) flexibility, (3) light transmittance, and (4) a high fiber content (~70%). One of the major advantage of cellulose fiber is the very low coefficient of thermal expansion (CTE) in the axial direction (0.1 ppm K^{-1}) as compared to quartz, while for BC nanocomposites, the CTE is reduced to a significant extent (~6 K^{-1}) with a fiber content of 70%.[33] This makes it possible to access transparent nanocomposites of cellulose obtained from bacteria, which represents a potential innovation for electronic device design.[27] BC has promising tensile behavior and toughness, which means that BC nanocomposites can be easily folded (Fig. 3(a)). When an electroluminescent layer is deposited on a transparent BC nanocomposite (Fig. 3(b)), a sufficiently low CTE can be achieved, but not enough flexibility.

Such an in-plane layered BC network creates a unique assembly of cellulose nanofibers with a minimum-bending radius, which offers distinctive properties for multiple applications. Optically transparent network construction is an area of major promise, where nanofiber-network-reinforced polymer composites are attractive transparent materials. At the same time, cellulose-microfibril-based resin and epoxy composites of BC have attracted major interest as materials with a high fiber content

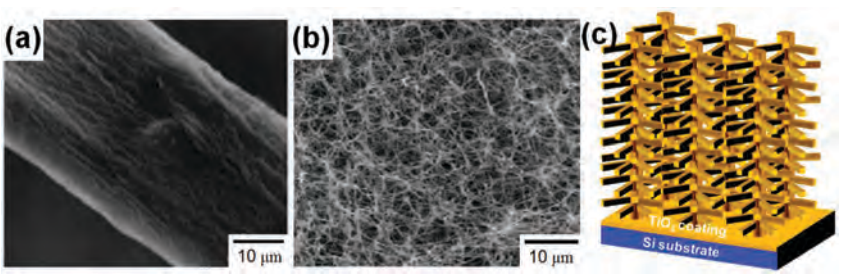

Fig. 2 3D nanostructures of a CNF obtained from common pulp from: (a) plant cellulose and (b) bacterial cellulose (reproduced from ref. 37, Wiley-VCH, 2012), (c) TiO_2 nanorods uniformly grown on dense Si nanowire (NW) array backbones to form a 3D NW architecture for implementation as an electrode photoelectrochemical cell (reproduced from ref. 39, American Chemical Society, 2011).

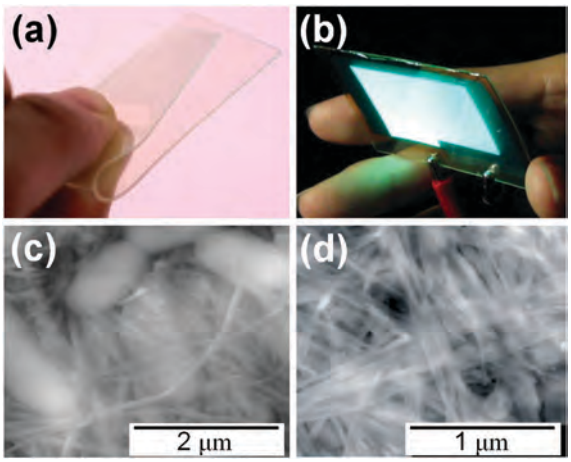

Fig. 3 (a) Digital image of a folded BC nanocomposite, (b) an electroluminescent layer deposited on the BC nanocomposite to obtain a low CTE. (Reproduced from ref. 27, Copyright Wiley-VCH, 2008.) (c) Atomic force microscopy (AFM) image, in tapping mode, of a BC pellicle, (d) the same BC/epoxy-resin sheet (reproduced from ref. 33, Copyright Wiley-VCH 2005).

and flexibility, as shown in the tapping mode AFM image of a BC pellicle in Fig. 3(c) and in the BC/epoxy-resin sheet in Fig. 3(d).[33] This is due to aggregation of the cellulose microfibrils, which extends them into semi-crystalline cellulose chains, and with a small thermal expansion coefficient similar to glass. In addition to single nanofibers with their excellent mechanical properties, web-like structures of nanofibers can further enhance the mechanical features of a matrix in which the fibers are embedded. Thus, BC nanofibers can act as reinforcing agents for many applications.

Dried BC aerogels with highly interconnected nanofibers with junctions (Fig. 4(a)), formed through self-assembly in bacteria culture, can be pyrolyzed to obtain 3D networks of carbon-based aerogels with reduced fiber diameters (Fig. 4(b)). These are highly promising for their scope of applications in energy storage in supercapacitors, artificial muscles, and gas sensors due to their low density, high electrical conductivity, porosity, and high specific surface area.[32] Such materials possess high electronic conductivity even under high stretching and bending strain. To obtain flexible and ultrahigh fire-resistant carbon nanofiber aerogels, BC offers macroscopic CNFs, which possess fire-resistant features along with a potentially high absorbance potential for pollutant oils, which makes them a suitable candidate for environmental applications, such as oil spill problems in the sea, as demonstrated in Fig. 4(c) in a gasoline-uptake experiment.[32]

As a unique class of fibrous cellulose, BC is an ecofriendly biomaterial with superior properties and is produced by various microorganisms (*Acetobacter xylinum*, *Pseudomonas*, *Rhizobium*, *E. coli*, *etc.*), and consists of ribbon-shaped ultrafine interconnected nanofibers with widths of less than 100 nm.[30,31] Thus, BC has a specific ultrafine network structure and particularly notable properties, such as sufficient porosity, high tensile strength, high water retention capability, and excellent biodegradability. Due to its incredible physical and chemical properties, BC has the ability to act as a 3D hybrid carbon nanomaterial for optically transparent films[33] and flexible optoelectronic devices.[44,45] Currently, several research groups have explored combining BC with conducting polymers (polyaniline, polypyrrole), by depositing them on BC nanofibers by an *in situ* polymerization of the aniline or pyrrole, with the aim of achieving completely renewable, biodegradable, and electroconductive composite materials. When used as a supercapacitor electrode, mass-specific capacitances of 273 F g^{-1} and 316 F g^{-1} at 0.2 A g^{-1} were achieved, respectively. Thus, the BC membrane has shown great potential as a substrate for flexible supercapacitors. The hydrophilicity of BC paper can be helpful for the contact between electrodes and aqueous electrolytes, and it can also provide diffusion channels for electrolyte ions, thus improving the supercapacitor performance.[46] BC, a typical biomass material, is composed of interconnected networks of cellulose nanofibers,[32,33] and can be produced in large amounts in a microbial fermentation process. Recently reports on a highly

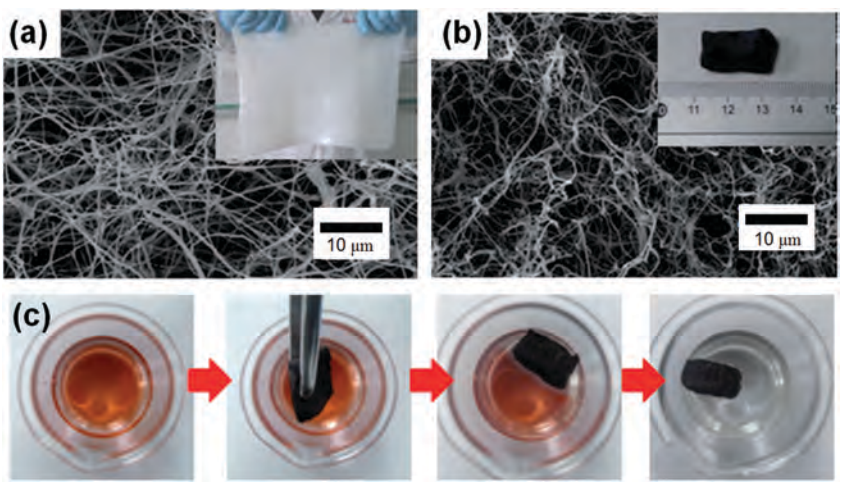

Fig. 4 SEM images of BC (a) and CNF (b) aerogels (inset to (a) shows the BC pellicle, and the inset photograph in (b) shows the size of the aerogel), (c) from left to right, uptake of organic liquids by a CNF aerogel (reproduced from ref. 32, copyright Wiley-VCH, 2013).

conductive and stretchable conductor, fabricated from BC showed that it had great electromechanical stability under stretching and bending strain.[33] BC nanofibers obtained from *Acetobacter xylinum* can reinforce polymer resins while maintaining the transparency of the original resin, even at a fiber content as high as 70 wt%, because the nanofibers do not appreciably scatter visible light. Flexible plastic composites reinforced with this renewable resource had thermal expansion coefficients of 6×10^{-6} °C^{-1}, a Young's modulus of 20 GPa, and tensile strengths reaching 325 MPa.[33]

3. Current strategies of cellulose nanofibril production

3.1. BC-based advanced nanostructures

BC has long been used as a raw material for Nata de coco, an indigenous dessert food of the Philippines, for which one-centimeter thick gel sheets fermented with coconut-water are cut into cubes and immersed in sugar syrup.[36] BC can be produced in large amounts on an industrial scale *via* a microbial fermentation process.[18,19] It is well known that BC pellicles are composed of interconnected 3D networks of nanofibers that have a native cellulose I crystal structure with high-molar-mass, hydrogen-bonded polymer chains in an extended-chain conformation.[27] The fiber content is structured in a web-like network, consisting of continuous nanofibers about 10 nm thick and 50 nm wide (Fig. 5(a)). The advantages of this fibrous network have been essentially captured in pyrolyzed BCs (Fig. 5(b)), which contain fibrous porous network structures that make them suitable for use as lithium battery anode materials.[47] In addition, BC has been used as a precursor material to prepare graphitized films[48] and carbon nanofibers from BC aerogels with a highly porous network structure consisting of numerous nanofibers with a diameter of 20–50 nm and that are highly interconnected with a large number of junctions (Fig. 5(c) and (d)).[37,47,49] When pyrolyzing BC-film at ~2900 °C, the original fibrous nature disappears in the BC-film, as revealed from the electron microscopic image in Fig. 5(d).[48] However, even by causing a decrease in the fiber diameter *via* pyrolysis, PBC aerogels are transformed to a 3D network structure (Fig. 5(e)) due to carbonization, which imparts excellent mechanical and conducting features to the PBC aerogels.

One of the most inspiring materials for the construction of 3D conductive carbon nanofiber networks involving BC as a precursor material for the fabrication of stretchable conductors comprises flattened double-walled carbon nanotubes (FDWCNTs) and epoxy in a layered-composite, which demonstrates superior mechanical properties (Fig. 6).[37] Examination of the FDWCNT/epoxy composite indicates that the layered structure is maintained, and that the orientation of the aligned FDWCNTs is retained during the fabrication process, in which many layers of FDWCNT/epoxy are held together to form a thin-film composite (Fig. 6(a)). Most nanowires consist of DWCNT bundles with excellent alignment and stacking along the direction of stretching, which was apparent from a drawn cross-section of the FDWCNT film (Fig. 6(b)), as compared to that of the non-flattened DWCNT. In the case of FDWCNT/epoxy composites, which maintain a layered structure and orientation during fabrication, these exhibit many layers held together to form thin-film composites with a thickness of each layer of ~100 nm at the secondary level, as shown in a drawn representation of the secondary structure of the bioinspired layered FDWCNT/epoxy composites in Fig. 6(c). Similarly, the construction of 3D conductive carbon nanofiber networks from BC pellicles for fabricating stretchable conductors also includes a multi-walled carbon nanotube (MWCNT)-incorporated BC membrane (Fig. 6(d)), with the corresponding TEM image shown in Fig. 6(e).[50] Thus, the insertion of MWCNTs into the BC pellicle is essential for a dramatic enhancement of the conductivity. This composite features a morphology with two different domains that can be easily distinguished, a continuous network of cellulose microfibrils, and the incorporation of MWCNTs distributed among them.

The major advantages of using BC as a precursor material include easy fabrication, low cost, and mechanical robustness of the 3D network structures, which is a key point for assuring the electromechanical performance of the final composites. As revealed, BC pellicles can be employed as starting materials for fabricating stretchable conductors, where pyrolyzed BC

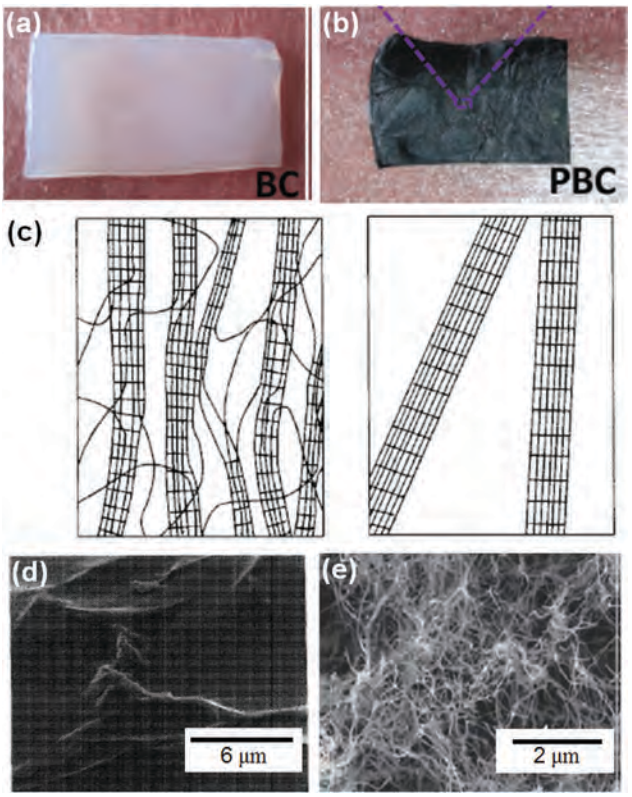

Fig. 5 (a) Pristine BC-pellicle, (b) pyrolyzed BC (PBC) aerogel after freeze-drying and pyrolysis (reproduced from ref. 47, Copyright Wiley-VCH, 2013). (c) Schematic model of BC microfibrils (right) drawn in comparison with "fringed micelle" (left), (d) SEM image of a heat-treated BC film (reproduced with permission from ref. 48, Copyright AIP, 1990), (e) and PBC aerogel obtained from pyrolysis of a BC aerogel (reproduced with permission from ref. 49, Copyright Nature Publishing, 2012).

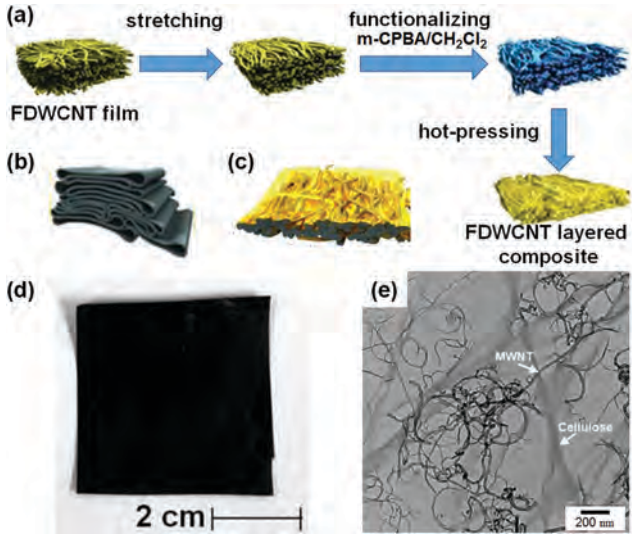

Fig. 6 Schematic illustrations of: (a) the fabrication of a bioinspired layered FDWCNT/epoxy composite with a cross-section of the aligned FDWCNT film, (b) one layer of the FDWCNT/epoxy film, and (c) the secondary structure of the bioinspired layered composite (reproduced with permission from ref. 50, Copyright Wiley-VCH, 2012). (d) MWCNT-incorporated bacterial cellulose pellicle, and (e) its TEM image (reproduced with permission from ref. 52, Copyright American Chemical Society, 2006).

(PBC/polydimethylsiloxane (PDMS)) composites exhibit high conductivity and extraordinary electromechanical stability, even under high stretching and bending strain.[37] As a special kind of cellulose, BC is produced by the fermentation of bacteria (*Acetobactor xylinum*, *E. coli*, *etc.*) in static or agitated culture. Although sharing a similar molecular structure to natural cellulose, BC has attracted ever-increasing attention as a bioscaffold, owing to its specific ultrafine network and specific surface properties, such as sufficient porosity, high purity, and crystallinity, as well as its promising mechanical properties, high water holding capability, excellent biodegradability, and biocompatibility.

Taking advantage of the net-like structure of BC with requisite porosity, hygroscopicity and hydrophilic wetting enhance ion transportation of the electrolyte. All biomaterial supercapacitors are constructed by the modification of a BC gel electrolyte, together with thermal treatment to obtain the electrode material.[51] These electrode materials from BC exhibit ion mobility with reasonable charging–discharging behavior and rate performances, thus paving the way toward obtaining electrodes made only of biomaterials for energy storage applications.

3.2. BC-conducting nanocomposites

Nanostructured-conducting-polymer–cellulose composites offer superior performance for many potential applications, such as batteries, sensors, antistatic coatings, and electrical devices.[52–54] The most common cellulose scaffolds for the preparation of polymer–cellulose conducting nanocomposites include cellulose pulp,[55] cellulose derivatives,[56] cotton cellulose,[57] microcrystalline cellulose,[58] and the BC membrane.[59,60] Due to its biocompatibility and water retention properties, BC has been a promising candidate for developing bioactive composites, especially for the production of bioactive wound dressings.[19] Such approaches have been extended for BC to form artificial blood vessels for microsurgery and for tissue regeneration and dental applications, which essentially aim to combine the possibility and versatility of compositions of hydrocollloids with the biocompatibility and structural characteristics of BC.

Among the conducting polymers, polyaniline (PANI) is one of the most promising candidates because of its facile synthesis, simple doping/de-doping chemistry, and controllable electrical conductivity.[61–63] BC/PANI as a conducting nanocomposite was first prepared by the *in situ* polymerization of aniline nanoparticles on a BC membrane, and exhibited a conductivity ranging from 1.61×10^{-4} to 1.3 S cm^{-1}. The low conductivity was due to the poorly controlled morphology of the composites using BC membrane as scaffold, but this can be further be improved by using BC nanofibers as the scaffold. Furthermore, in order to further improve the conductivity and capacitance performance of cellulose–PANI or other conducting polymer nanocomposites, first determining the growth mechanism of PANI on the BC scaffold is essential. The flake-like morphology of BC/PANI nanocomposites, obtained by altering the ordered flake-like structure, achieved outstanding electrical conductivity, as high as 5.1 S cm^{-1}, with a mass-specific capacitance of 273 F g^{-1} at 0.2 A g^{-1} current density for supercapacitor application.[31] It is very important to focus on the nature of the interactions between the PANI coating and the BC nanofiber substrate to elucidate the reason for the high conductivity. X-ray photoelectron spectroscopy (XPS) analysis of the PANI–BC composite suggested that it may be due to hydrogen bonding interactions of nitrogen lone pairs (N) of the polymer coating with –OH groups of the cellulose substrate. The most distinct morphology change that occurs is that the fiber-like morphology is transformed to a flake-structured with a high densification and aggregation of BC/PANI flakes, mainly due to the hydrogen bonding between PANI layers. When comparing the structural morphology of the PANI–BC composite with the supercapacitor performance, the *in situ* polymerization of PANI and the coating of PANI layers onto the BC nanofibers to form core–shell structures were both important. This process involved: (a) aniline dispersion and self-assembly on BC nanofibers with dimethylformamide (DMF) assistance and (b) the *in situ* polymerization of aniline with ammonium persulfate (APS), together with doping by HCl. The results indicate that the BC/PANI nanocomposite had an obvious capacitance performance, with a pair of Faradaic peaks relating to the protonation/deprotonation processes. One of the key features missing in this system is that the inadequate porosity is reflected in the non-rectangular shaped CV curve, thus preventing it achieving a high performance. This suggests that there is more scope to improve the morphology as desired for improved capacitance performance.

For further understanding the role played by the conducting polymer layer on BC for charge storage application, core–shell structured conductive nanocomposites, for example, a homogeneous polypyrrole (PPy) applied in a layer around BC nanofibers *via* the *in situ* polymerization of self-assembled Py,

was considered as suitable candidate. The composite exhibited an electrical conductivity of 77 S cm^{-1} at an optimized mass ratio (BC/Py 1 : 10) and a promising mass-specific capacitance (316 F g^{-1} at 0.2 A g^{-1}). For constructing the morphology of PPy@BC, hydrogen bonding plays a major role in the densification and aggregation in an aqueous medium, resulting in a BC–PANI with 86 wt% PANI from an aqueous medium (Fig. 7(a)), while the weakening of such intermolecular interactions *via* DMF results in separated homogeneous BC@PPy fibers.[64] The improved dispersion of pyrrole in the miscible DMF–H_2O mixed solvent makes the evolution of the PPy@BC morphology different from that of the nanofibrous BC/PPy membranes in aqueous medium,[65] in which, for the former, a uniform coating of PPy layers wrapping the BC nanofibers occurs. The weakening of the intramolecular H-bonding-driven interactions *via* DMF solvation results in separated and homogeneous BC/PPy fiber nanocomposites through the optimized addition of Py, $FeCl_3$, and HCl at 0 °C in various biphasic media (Fig. 7(b)–(d)).[64]

The XPS spectra show that the core levels of C 1s and O 1s for the BC fibers are shifted to higher binding energies due to both the shielding effect of the PPy sheath and the strong interactions between PPy and BC, such as the hydrogen bonding between the nitrogen lone pairs (N) of the polymer coating with the –OH groups of cellulose. This makes the BC/PPy core–shell composite electrode highly electrochemically stable, retaining about ~88.2% of the initial capacitance after 1000 cycles. Retention of the important redox feature of the conducting polymers in the nanocomposites is supported by the rectangular cyclic voltammetry (CV) traces, showing a high degree of electroactivity, with an electrochemical redox reaction at the interface between the electrode and electrolyte involving PPy. The discharge capacitance (C) is 316 F g^{-1} at 0.2 A g^{-1}, which is much higher than that of cellulose–nanocrystal/PPy porous composites, while the performance of the *Cladophora* cellulose/PPy composites can be attributed to the core–sheath-structured BC/PPy, which has a thick (80 nm) PPy layer wrapped homogeneously around the BC nanofibers that provides a larger electrolyte-accessible conductive surface for the redox reaction than for other BC/PPy composites.[66–68] A further development of BC-based composites depends on the production of hydrocolloid films and the preparation of biocompatible collagen surfaces. Understanding the surface properties of the resulting materials, especially the factors that determine cell adhesion and proliferation in the bionanocomposite surfaces, will have a major effect on the ultimate success of biocompatible BC-nanocomposites.

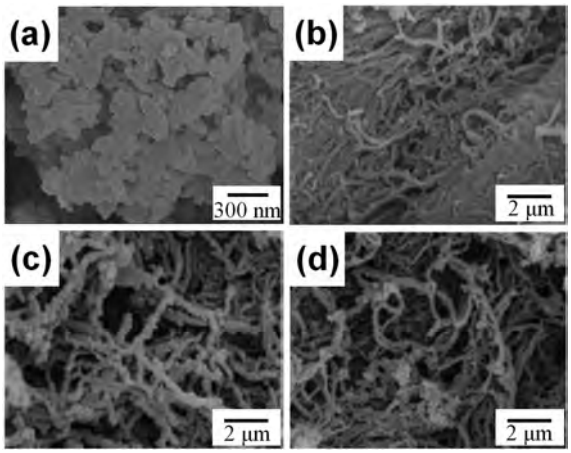

Fig. 7 (a) FE-SEM image of a BC/PANI nanocomposite with 86 wt% PANI prepared from pure water (reproduced with permission from ref. 31, Copyright American Chemical Society, 2012). (b–d) FE-SEM images of PPy/BC nanocomposites prepared with the optimized addition of Py, $FeCl_3$ and HCl at 0 °C in (b) pure water, (b) DMF–H_2O (1 : 1, v/v), and (d) DMF–H_2O (3 : 2, v/v) (reproduced with permission from ref. 64, Copyright Royal Society of Chemistry, 2013).

3.3. BC-paper electrodes

Papers are suitable candidates for substrates in flexible energy storage applications due to their natural tendency to integrate with conductive materials, such as carbon nanotubes. In general, BNC fibers smaller (20–100 nm) than those of conventional cellulose fiber (~10 μm) are considered suitable for paper electrodes. Owing to the reduced size of BNC fibers, BNC papers can be made thinner, yet their mechanical strength can still be higher than that of regular papers. Indeed, it is the superior mechanical strength and stability of BNC papers that would make them more compatible with the electrochemical conditions under which supercapacitors operate.[39,69] Flexible electronics contain electrode materials that outperform conventional activated carbon for supercapacitor application. For example, carbon nanotubes (CNTs) ensure high flexibility, while providing long, continuous conductive paths and they are also capable of coating a rough surface, such as paper, which ensures high integrity.

The fabrication of solid-state flexible supercapacitors based on BNC, CNTs, and ionic-liquid-based triblock-copolymer gel electrolytes has been a successful strategy to date, and the supercapacitors produced have shown excellent cyclability over 5000 charge/discharge cycles at a current density of 10 A g^{-1}. Rational design is involved in constructing such flexible supercapacitors with BNC and is indeed highly important, as it depends on the purity (free of hemicellulose, lignin, and other extraneous materials) and high crystallinity, which enables the high tensile strength of the BNC fibers.[43] BNC/CNT/ion gels, depending on the interfacial quality between the three different layers, can be used to construct excellent flexible supercapacitors that can form the basis of advanced flexible energy storage devices.[70] To form such flexible supercapacitors, a CNT layer was deposited onto BNC paper *via* a vacuum filtering process depending on the interfacial properties (H-bonding and van der Waals interactions), and the resultant CNT-coated BNC paper exhibited excellent mechanical stability. BNC fibers and CNTs have similar 1D structures that are intertwined into two-dimensional (2D) sheets (Fig. 8(a)). This system also featured a seamless interface between the CNT and BNC layers, ensuring good mechanical integration between the two different materials (Fig. 8(b)). In addition, a high quality interface results from the similar 1D geometry of the CNTs and BNC fibers, which can be easily integrated due to the strong forces, such as van der Waals

interactions and hydrogen bonding, between the two layers (Fig. 8(c) and (d)).

3.4. Carbon aerogels

Carbon aerogels consisting of 1D carbon nanofibers with high aspect ratios due to their highly aligned intersected structure offer adsorptive and conductive properties. Unlike porous carbon aerogels from renewable biomass wastes, BC, with its high content of superfine nanofibers (40–60 nm), large specific surface area, and high crystallinity, essentially offers nitrogen-doped carbon networks *via* coat of PANI and polyamide on BC. Carbon-nanofiber-based aerogels with desired mechanical properties are in demand; however, the lack of strong cross-linking in BC-derived nanofibers results in their poor shape-retention. A strategy of obtaining carbon aerogels consisting of 1D-carbon nanofibers (BC-derived) and a 3D-carbon skeleton (from polyimide (PI)) was established *via* sequential imidization and carbonization.[71] These carbon aerogels were versatile and had superior adsorption and energy storage abilities. With the increase in PI content, the compressive modulus of BC/PI aerogels was improved, which was due to the presence of rigid chains of polyimide and enhanced cross-linking between the polyimide and ultrafine BC nanofibers. This results in excellent mechanical properties, which promote the strategy of making carbon aerogels from BC by incorporating suitable cross-linker, which results in a 3D-interconnected microstructure that imparts robustness in aerogels with low density. This 1D carbon nanofiber (from BC) and 3D carbon skeleton interpenetration results in a porous network that offers capacitive behavior of the electrode with reduced impedance.

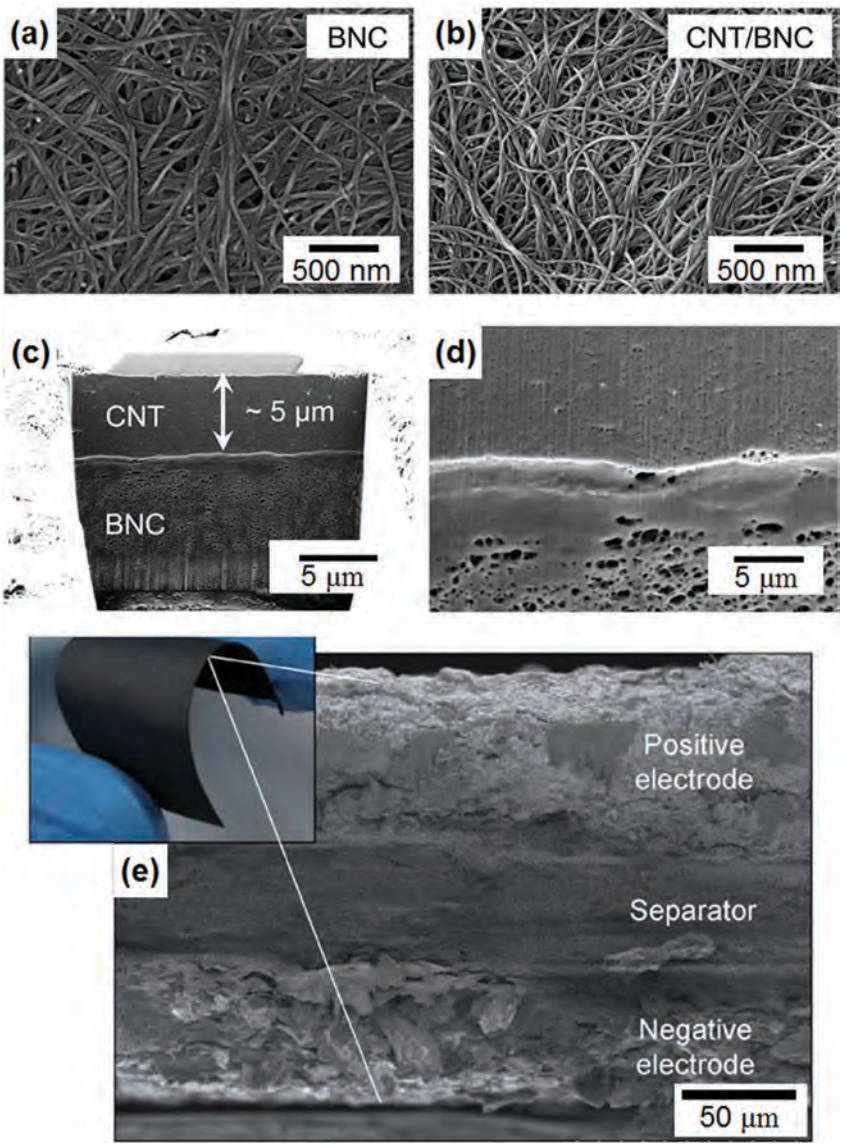

Fig. 8 (a) CNTs coated on BNC paper: (b) cross-sectional view of a CNT/BNC paper, (c and d) magnified SEM image of the interface between the CNT layer and the BNC layer (reproduced with permission from ref. 70, Copyright American Chemical Society, 2012). Illustration of flexibility of a paper battery (inset) of the SEM image of a paper battery cross-section (e) (reproduced with permission from ref. 82, Copyright Royal Society of Chemistry, 2013).

Cellulose-derived carbon aerogels feature not only a small environmental footprint, but can also offer reversible compressive deformation and areal capacitance due to their mesoporous framework, which in turn is excellent for their use in flexible energy storage devices.[72] A highly graphitized carbon aerogels based on BC nanofibers and a lignin–resorcinol–formaldehyde polymer offers excellent areal capacitance, which can be further enhanced by introducing a microporous network. Some of the potential applications of carbon aerogels derived from cellulose and lignin include the absorption of oil for oil/water separation, supercapacitors, batteries, catalyst supports, and a sensor, while the large mesoporous framework for the transportation of ions and reversible deformation due to the interpenetrated networks of composite are two key features.

3.5. Hybrids of CNF and carbon nanomaterials

Electrolyte ion-diffusion phenomena can be facilitated by constructing porous hybrid microfibers of CNF with a carbon nanostructure, such as single-walled carbon nanotubes (SWCNT). In this case, SWCNTs were found to orient along the axis direction of the microfiber due to an induction of the extrusion (Fig. 9).[73] This enables electron transport along the axial directions. CNF also prevents the possibility of the aggregation of the SWCNTs and improves the re-swell properties of the microfiber in aqueous electrolyte due to the high hydrophilicity. Such a hybrid nonwoven microfiber mat contains a reservoir of electrolytes, whereby the CNFs can absorb electrolytes, which facilitates electrolyte diffusion. The CNF-based hybrid electrode holds promises, like other CNF or BC-derived carbon nanostructured hybrid electrodes, when decorated with metal oxides or metal nanoparticles.

Carbon nanofiber composites in the form of carbon-nanofiber aerogels and transparent composites are good candidates for constructing asymmetric supercapacitors to obtain a reversibly charged device. For such a system, hybrids of CNFs derived from BC are key candidates for achieving ultrahigh energy and power densities as Faradic electrodes. For replacing carbon-containing asymmetric supercapacitors in a relatively cost-effective way and for obtaining high operation voltages, hybrids of CNF, especially CNFs derived from BC, are worth exploring. In this direction, BC pellicles (p-BC) composed of interconnected nanowires have been employed to construct macroscopic-scale carbon-fiber aerogels and transparent composites.[74] An asymmetric supercapacitor composed of a 3D p-BC nanofiber-network-coated MnO_2 (p-BC@MnO_2) was used as a positive electrode, alongside a negative counterpart consisting of p-BC/N. This optimized device could be reversibly charged/discharged at a voltage of 2.0 V with a high energy density of 32.91 W h kg^{-1}. For a redox Faradic reaction, the pseudocapacitance of MnO_2 determines the Faradic reactions on the surface, and thus, the film of MnO_2 formed on the CNF provides a highly electrochemically active component with the MnO_2 nanofilm. This ensures effective reduction of the diffusion length of the electrolyte (Na_2SO_4) ions during the charge/discharge process for the rapid reversible Faradic redox process.[75]

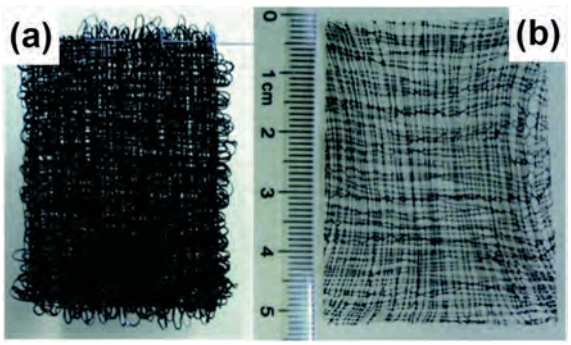

Fig. 9 Digital photograph of the wet (a) and dry (b) CNF/SWCNT hybrid microfiber mat used as supercapacitor electrodes. (Reproduced from ref. 73 with permission from Royal Society of Chemistry, Copyright 2014.)

3.6. Wood cellulose fiber

By possessing natural unique hierarchical and mesoporous structures that can enable a variety of new applications beyond traditional domains, wood fibers are a potential candidate for not only transparent and clear paper materials,[76] but also for wood-fiber-derived porous carbon electrodes.[77] The random network of wood fibers modulates the propagation of light when the wood fibers form a highly transparent and clear paper (transmittance $>$ 90%). Transparent cellulose paper originating from mesoporous wood fibers offers compatible optical properties for replacing plastic substrates, while the comparable device performance is an incredible step toward an emerging new class of photonic materials. The major issue with these materials relates to how the hierarchical structure of wood fibers, where microfibers are composed of nanofibers, is used for deriving natural fibers. From hierarchical fibers, super clear (transmittance $>$ 90% haze $<$ 1%) and super hazy (transmittance $>$ 90% haze $>$ 90%) papers can be derived. The thermal carbonization of wood fibers modified by 2,2,6,6-tetramethylpiperidine-1-oxyl (TEMPO), which effectively reduces the surface area of porous carbon electrodes, imparts excellent cycling stability, which is important for a promising anode. The incorporation of TEMPO layer formation resulted in densely packed wood fibers, which was in sharp contrast with the porous configuration of pristine wood fiber. Pristine carbon paper contains many nanosized pores, but TEMPO treatment leads to a less porous surface for the resulting carbon paper. Thus partial unzipping of the wood fibers with TEMPO creates ribbon-like structures with a higher packing density and lower surface area.

Various types of cellulose nanofibrils, and their significant structural features and potential applications are summarized in Table 1, which can be used to help in determining the strengths and drawbacks of different approaches for constructing the components of electronic devices centered on cellulose-derived composites. For example, most carbon aerogels are based on carbon nanotubes (CNTs) or graphene, although these can be replaced with biomass-based organic aerogels that feature low cost, high scalability, and a reduced environmental footprint. What is more revealing is that in most cases, cellulose-derived composites were found to be superior as compared to conventional materials in certain ways. Carefully selected references in this area describe such advantages, and herein, we attempt to offer a comparative insight into the critical features of cellulose-derived

composites for their applications. For example, organic resorcinol–formaldehyde (RF) or lignin–resorcinol–formaldehyde (LRF) aerogels are brittle and fragile, but they can be toughened by using BC. This process offers highly graphitized carbon nanofibers with large mesopores and 20% reversible compressive deformation. As a suitable candidate for flexible electronics, the BC-modified carbon LRF offers higher areal capacitance (maximum 124 F g^{-1}) as compared to activated carbon.[72] High physical flexibility and excellent mechanical integrity were also achieved by exploring bacterial nanocellulose-, carbon nanotube-, and ionic-liquid-based three-layered polymer gel electrolytes. This BC-paper-based composite achieved a maximum specific capacitance of 50.5 F g^{-1} with a minimum reduction in capacitance (<0.5%) over 500 charge/discharge cycles at a current density of 10 A g^{-1}.[70] A BC–poly(amic acid) composite consisting of 1D carbon nanofibers and a 3D carbon skeleton offered a high specific capacitance of 194.7 F g^{-1} due to its interconnected pores for fast ion diffusion, efficient charge sorption, and rapid electron transport.[71] Thus, a multidimensional carbon composite derived from BC not only outperformed a series of carbon-based electrodes, including BC and graphene-based composites, but also revealed a new trend toward using multidimensional carbon aerogels for a wide-range of electrochemical applications. It has also been realized that among the many cellulosic sources offering porous electrode platforms for making composite electrodes, BC, consisting of a high content of superfine nanofibers (40–60 nm diameter) free of lignin/semicellulose, exhibits a large surface area, and high crystallinity and porosity. For next-generation carbon-nanofiber-based aerogels with excellent mechanical properties, however, strong cross-linking bonds/sites between BC and the derived carbon nanofibers represent the key to improving the shape-retention capability.

4. Cellulose-derived composites in energy storage

The research within the field of energy storage devices has undergone significant evolution toward upgrading to achieve flexibility and cost minimization, and in this area, cellulose-based composites/paper devices are being developed with a particular emphasis on flexible paper-based batteries and supercapacitors.[78] The major advantage of the cellulose-based composites is their high theoretical capacitance due to the presence of Faradic reactions and double-layer charging.

4.1. Lithium-ion batteries

The requirements that have to be met by rechargeable batteries (metal-ion batteries) in terms of power density, energy density, and cyclability have stimulated the direction of current investigations toward a new dimension for achieving high-performance components of electrodes from renewable sources.[79,80] Cellulose is one of the most abundant renewable natural polymers, and serves as precursor to form carbonaceous materials that can be applied for energy storage, carbon fiber fabrication, water purification, ion exchange, catalysis, and electronics. High-temperature carbonization and hydrothermal carbonization are two established techniques used to acquire carbonaceous materials from cellulose, even though the carbon structures obtained by these methods exhibit low conductivity. Thus, a necessary requirement is to develop strategies to enhance the conductivity of carbonized materials by improving the graphitic structure of the carbonized product, which essentially means enhancing the order of the graphene stacks.

Cellulose undergoes thermal cleavage of the glycosidic linkage,[81] scission of the ether bonds, and depolymerization to macrosaccharide derivatives, finally forming the desired carbon structures after releasing gases containing the non-carbon

Table 1 Summary of the different cellulose-nanofibril types, their structural features, and potential applications

Entry	Cellulose material	Structural features	Applications
1[49]	BC-based advanced nanostructures Flattened double-walled carbon nanotube (FDWCNT)/epoxy fiber composite	Layered hierarchical nano-micro structure of an epoxy-based composite with higher mechanical strength	Mechanical applications due to improved strength as compared to epoxy-based composites
2[64]	BC-conducting nanocomposites PPy/BC nanocomposite	Core–sheath structure with a PPy coating on a BC nanofiber core	Supercapacitor electrodes
3[70]	BC-paper electrode CNT/BNC/ion-gel	BNC fibers and CNTs have similar 1D structures that are intertwined into 2D sheets	Solid-state flexible supercapacitor, supercapacitor with ion gels
4[73]	CNF/SWCNT hybrid nonwoven microfiber mat	SWCNT preferentially oriented axially along the microfiber due to the extrusion process, uniform microfibers, porous structure, and electron transport along the axial direction	Hydrophilic and re-swelling features, both electrode materials and charge collectors can be used as wearable components of supercapacitors
4[71]	Carbon aerogels from BC/poly(amic acid) composite	1D carbon nanofibers and a 3D carbon skeleton, interconnected pores, cross-linked structure	Excellent compressive properties, adsorbents, sorption capacity, recycling ability, supercapacitor electrodes
5[72]	BC-modified lignin–resorcinol–formaldehyde (LRF) aerogels	Core–shell structure, reversible compressive deformation, large mesopore population	High areal capacitance, flexible solid-state energy storage in supercapacitors, sensors, oil–water separation
6[76]	Wood cellulose fiber	Random network, transparent mesoporous, hierarchical pore structure (micrometer to nanometer), the pores can be filled with high index materials to create periodic photonic structures, the packing of the cellulose fiber can be find tuned	Photonic and optoelectronic application, flexible electronics

atoms (O, H). Paper-battery cells can be produced at low cost by using existing paper-making procedures. Nano-fibrillated cellulose (NFC) acts as a binder material as well as a load-bearing material, and thus offers several advantages over more conventional cellulose fibers, while its nanoscale dimension also allows incorporation in nanostructured devices. The clear difference between NFC fibrils (5–30 nm wide) and cellulose fibers (20–30 μm) is that NFC overcomes the limits to the performance of cellulose-fiber-based separator films in terms of thinness and acts as an efficient binder material on the nanoscale. One potential danger from integrating electrodes and the separator in a single unit, especially when the constituents are in the form of dispersions during the manufacturing process, is short-circuiting. This might occur either by the formation of an electrical conducting tunnel through the separator layer during the filtration process, or by an overlapping of the two electrodes at the edges of the battery paper. This method of making flexible and strong battery cells enables full control over the active material loadings of the electrodes by controlled additions from the respective water dispersions.[82] After drying under vacuum, thin (250 nm) and flexible paper batteries can be formed (Fig. 10(a)). A scanning electron microscopy (SEM) image of a paper-battery cross-section shows three discrete and well-adhering layers, comprising the three battery components (Fig. 10(b)). Making this mechanically bendable battery from nanofibrillated cellulose is useful for a wide variety of new applications. Ecofriendly cellulose nanofibers can be successfully explored as a separator for LIBs.[83] The cellulose/poly(vinylfluoride-*co*-hexafluoropropylene) composite is one example that can be fabricated as an advanced nonwoven separator for high-performance LIBs *via* the electrospinning technique and dip-coating.[84] Commercial polyolefin separators for LIBs can be effectively replaced by tuned-porous-structured CNF-based separators *via* a facile fabrication technique based on structural control through colloidal SiO_2 nanoparticles.[85] To address the safety concerns about LIBs, the current challenge is to develop a heat-resistant and flame-retardant cellulose separator. The cellulose-based composite nonwoven separator, with its great flame-retardant and electrochemical characteristics, represents an important advance, *via* the strategy of replacing the synthetic polymer by a renewable polymer-derived separator that essentially features higher porosity (~15%). The highly porous structure of the flame-retardant cellulose-based composite nonwoven (FCCN) separator results in high electrolyte uptake, which leads to high ionic conductivity due to more electrolyte being soaked up by the FCCN separator, and this facilitates rapid ionic transportation.[86]

FCCN contains the following special features, which offer advantages over the polypropylene (PP) separator obtained from substituted polyolefins: (1) improved electrolyte wettability, (2) mechanical robustness and integrity, (3) uniform tensile strength, and (4) better cycling performance in LIBs with a stable charge/discharge behavior. These features in FCCN enable much better safety features, which essentially make the FCCN separator promising for LIBs for consumer electronics. These improved features of FCCN can be attributed to its highly interconnected micropores and the lyophilic nature of the cellulose fiber framework. The cellulose pulp-derived FCCN separator contains well-distributed

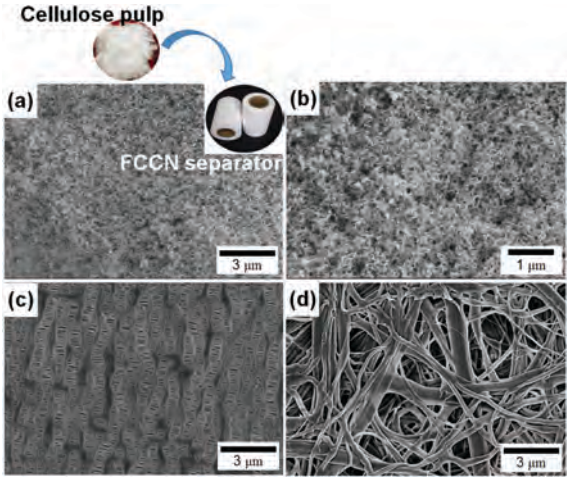

Fig. 10 SEM micrographs of (a) FCCN separator and (b) the same separator at higher resolution (2000×). SEM micrographs of (c) PP separator and (d) CN separator at the same resolution, featuring a large network of different sized pores (reproduced from ref. 86 with permission, Copyright Nature Publishing Group, 2014).

pores (100–200 nm) (Fig. 10(a) and (b)), which play an essential role in preventing internal short-circuits, avoiding self-discharge, and facilitating uniform current density at high charge/discharge rates. SEM micrographs of the PP separator (Fig. 10(c)) and CN separator (Fig. 10(d)) at the same resolution show that they feature large networks of different sized pores; however, whereas the PP separator showed uniform and typically elliptic pores, the CN separator showed excessively large size pores (>4 μm), making the CN-separator short-circuit prone during the charge–discharge process.

It is also very interesting that a specific structural type (*i.e.* a structure full of twists and turns) is more favorable for preventing the growth of lithium dendrites, which is essential for battery safety. It is thus essential to examine the electrochemical interfacial stability from this point of view, which can be guaranteed by use of the cellulose/poly(vinylidene fluoride-*co*-hexafluropropylene) (PVDF–HFP) composite separator as compared to the commercial PP separator,[86] as the interfacial compatibility of lithium metal with the separator plays an important role in lithium batteries for their application. The interfacial compatibility of a liquid-electrolyte-soaked separator made from nonwoven cellulose composites with a lithium metal anode can be determined by measuring the interfacial resistance between the lithium metal anode and the separator. At the same time, a thinner fiber diameter of the separator enhances the porosity, thus soaking up more liquid electrolyte, which essentially enhances the ionic conductivity to a great extent.[87]

Cellulose nanofibrils (CNFs) can act as superior reinforcing materials, either in composite structures[88] or together with a liquid electrolyte. It was demonstrated that, by using functionalized porous CNF nanopapers in composite electrolytes as a reinforcing phase in an ionically conductive polymer matrix, several issues related to the LIB performance could be addressed, including: (1) the difficulties associated with the phase migration, (2) changes in

the phase geometry, and (3) the post-functionalization of the fibril surfaces, which can improve the interfacial strength in the final composite electrolyte. When CNF is modified by an acid chloride to install acrylate and alkyl functionalities onto the surface and is then reacted with polyethylene glycol (PEG)-methacrylate, it results in covalent bond formation between the two functionalities and the alkyl groups, which keeps the number of unmodified OH-groups constant.[89]

Mechanically prepared CNF nanopaper surfaces were modified with acrylate and propionate to prepare composite electrolytes with modified and unmodified CNF. Compared to the unmodified CNF paper electrode, for samples with a large amount of acrylate groups, the ion transport capability was reduced due to the limited segmental mobility of the PEG segments. Strong fiber matrix interactions can offer moderate ionic conductivity as a consequence of the covalent bonds. These results, in terms of enhancement of LIB performance, confirmed that the conductive polymer was covalently attached to the CNF, thus emphasizing the importance of a strong interface with the electrode materials. The performance of this system in terms of the resulting currents was evidenced by the cyclic voltammograms, which give an indication of the relatively stable electrochemical behavior of the composite electrolyte. The most interesting feature of the microstructure of the composite electrolyte is that, while it has a matrix and covalent linking to CNF fibers, essentially no naked fibers can be detected. This suggests that strong interfaces play the major role in the composite electrolyte when it undergoes dimensional changes in the LIB environment. When the composites are subjected to dimensional changes in the LIBs, strong interfaces for the CNF are highly essential, as revealed from the SEM image analyses of the CNF (Fig. 11(a)) and wet CNF containing naked fibers (Fig. 11(b)).[89]

The fabrication of flexible electrodes from CNF is possible due to its high elastic modulus and low thermal expansion, so that it is capable of hosting a range of guests required for flexible electrodes.[90–94] The concept of recyclable device production was demonstrated by using CNF as a major component of a free-standing lithium titanate ($Li_4Ti_5O_{12}$ (LTO))/carbon nanotube/CNF hybrid network film, and it was stated that the ease of their assembly could facilitate the use of such films as easily-scaled-up alternatives.[95] The film represents a free-standing, flexible paper electrode using CNF as both a support skeleton and a binder. For this flexible electrode, LTO nanoparticles were used as an active material and CNTs as an electronic conductivity enhancer. The free-standing films as highly flexible paper electrodes have the following advantages: (1) robust conductive fibrous network, (2) electronic conductive paths due to CNTs, (3) increased contact area between CNT/CNF and good adhesion, and (4) high flexibility and a dispersive nature in aqueous medium. The major strategy in constructing a free-standing film is a pressure-controlled fast assembly of the LTO/CNT/CNF hybrid as a flexible paper electrode. High rate performance, high charge/discharge capacities, and good cycling stability emphasize the importance of building a skeleton for the free-standing film.

Flexible cellulose-based electrode materials generally are used in the form of a composite of nanostructured cellulose and PPy, constructed by the chemical oxidation of Py in the presence of cellulose extracted from green algae, which consists of cellulose fibers coated by a thin layer of PPy, in which the algal cellulose acts as a template for the PPy thin layer.[96] The rapid mass transport of ions needed during the oxidation and reduction of PPy with overall flexibility will be offered by the cellulose substrate. This metal-free battery device featuring PPy–cellulose composites as two electrodes, offers a charge capacitance up to a maximum of 48 mA h g^{-1} per total weight of PPy active material under a cell voltage of 1 V. In spite of certain factors, such as limitations due to the cellulose sources and the lower energy density of cellulose-based charge storage systems as compared to metal-based systems, cellulose composite-based paper electrode systems are suitable candidates where flexibility and environmental issues are prime factors. This invites more scope for exploratory research on cellulose-based paper electrodes, and more so for the options of replacing conventional electrodes with wood-cellulose-based electrodes, given the problem of stability and the self-discharge of electronically conducting polymer (ECP)-based batteries and supercapacitors.

From the above discussion, it is clear that, in spite of being inherently non-conductive, cellulose fibers are widely known for their mechanical strength and flexibility, which makes them suitable substrates for reinforcing conductive polymers and metal oxides and significantly enhancing their electrochemical properties. Some of the results discussed above in terms of the nanostructures of cellulose-materials can also be expressed in terms of their electrochemical performance (Table 2), together with their specific advantages over conventional materials and their limitations.

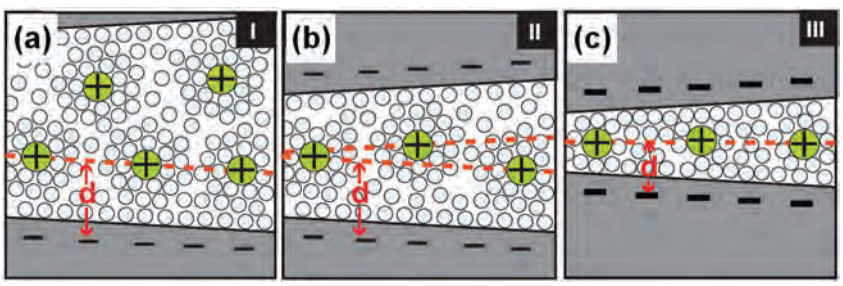

Fig. 11 Illustration of solvated ions residing in pores, with distances between the adjacent pore walls being: (a) greater than 2 nm, (b) between 1 and 2 nm, (c) less than 1 nm (reproduced from ref. 93, Copyright Science Publishing, 2006).

4.2. Supercapacitors

Electrical double-layer capacitors (EDLCs), often called supercapacitors, have steadily risen in importance as high power electrochemical energy storage devices with ultralong cycle life, sub-second charging, and a very wide operational temperature range. Even with these properties currently unattainable, Li-ion batteries are applied in devices, such as consumer electronics, uninterruptible power suppliers, electric and hybrid electric vehicles, and power grid applications. Electrically conductive porous electrodes with a large specific surface area are essential for the energy storage in EDLCs, based on the electrostatic adsorption of electrolyte ions. The greater cycling stability and higher electrical conductivity of porous carbons have led to their strong presence in the development of carbon-based supercapacitors. In this regard, the surface chemistry and pore size distribution of carbon materials play major roles. In principle, the ideal pores should be slightly larger than the size of the de-solvated ions, as smaller pores prevent efficient ion electrodesorption, whereas significantly larger pores reduce the capacitance. The negative effects of the larger pores are often witnessed during the carbon activation process. During carbon activation studies, the effects of pore size may be more significant during longer activation times for the carbon materials, where a resultant larger specific surface area (SSA) results in an increase in the capacitance. The negative effects of larger pores are revealed when the average pore size increases with a prolonged activation time. Earlier, energy storage in carbon-based EDLCs was modeled *via* the Helmholtz electrical double-layer (EDL), with solvated ions adsorbed onto the internal carbon pore surface. Systematic studies revealed that a significant enhancement of the specific capacitance in the small micropores could be achieved when the ion solvation shell becomes highly distorted and partially removed.[97] Studies of normalized capacitance behavior with varied-pore-size-based ionic transport of solvated ions showed that extremely narrow pore sizes (supercapacitors in hybrid vehicles) lead to longer discharge times, together with an energy density premium. Pictorial representations of solvated ions residing in pores, with the distances between the adjacent pore walls being greater than 2 nm (Fig. 11(a)), between 1 to 2 nm (Fig. 11(b)) and less than 1 nm (Fig. 11(c)) illustrate the variation in the normalized capacitance with the pore size.

Supercapacitors as electrochemical storage devices have drawn tremendous attention due to their high power density, long cycle lifetimes, and moderate energy density. In spite of significant efforts dedicated to developing them, flexible and lightweight supercapacitors still have more scope for many applications, such as portable electronic devices, displays, electronic paper, and stretchable electronics.[95] Several substrates have now been established as materials for flexible electrodes for supercapacitors, including paper, graphene paper, and polydimethylsiloxane.[97,98] The capacitance of an electrochemical capacitor is determined by two storage principles: double-layer capacitance and pseudo-capacitance, where both contribute to the total capacitance. Generally, these capacitors contain highly porous electrode materials with a large surface area, such as carbon nanotubes, activated carbon, and graphene, which contribute to the double-layer

Table 2 Electrochemical performance of cellulose-derived paper separators for LIB applications and comparison of the performances with conventional separators

Entry	Material	Features	Ion conductivity (mS cm^{-1}, σ_{eff})	Tensile strength (MPa)	Tensile modulus (MPa)	Interfacial resistance (Ω)	Thickness (μm)
1[83]	CNP (cellulose nanofiber paper)	Porous structure tuned with the disassembly of IPA–water	0.77	21	3257		19
2[83]	Commercial tri-layer (PP/PE/PP) (polyethylene/polypropylele)	Poor thermal shrinkage and weak mechanical strengths: full electrical isolation of electrodes is an issue	0.73	180	678		20
3[85]	S–CNP (silica-cellulose nanopaper)	Colloidal SiO_2 nanoparticle directed nanoporous S–CNP with loose packing of CNF with the evolution of more porous S–CNP	2.40		960		37
4[84]	Cellulose/PVDF–HFP composite nonwoven(poly(vinylidene fluroride-*co*-hexafluoropropylene))	Randomly arranged nanofibers with smaller pore size (100 nm) when PVDH–HFP is filled with cellulose nonwoven	1.04	33	960	180	27
5[84]	PP (polypropylene) separator commercial	—	0.64		240	340	25
6[86]	Flame-retardant and thermal resistant cellulose-based composite nonwoven (FCCN)	Pores of 100–200 nm prevent internal short-circuit, avoid self-discharge, and achieve uniform current density at high charge/discharge rates	2			170	40

A McMullin number (N_M) = σ_o/σ_s (σ_o ionic conductivity of liquid electrolyte and σ_s ionic conductivity of liquid electrolyte-filled separator).

capacitance.[99] One of the major problems for nanomaterial-based electrodes is the inaccessible surfaces of the electrode, which drastically reduces their actual capability for double-layered capacitance, thus reducing their specific capacitance. In this section, we aim to discuss recent developments and trends in employing cellulose-fiber-based composites as supercapacitor electrodes and their performance. Two major strategies that can make a difference are: (1) the use of cellulose fiber and BC as substrates for the deposition of energy storage materials, and (2) the incorporation of cellulose fiber in composites with electrochemical charge storage materials.

When cellulose fibers are used as a substrate for the deposition of energy materials, the obvious question that arises as to how this substrate can surpass the features of the existing electrode types obtained from conventional carbon sources. However, the cellulose fiber has unique features, such as: (1) higher absorption of electrolytes in cellulose fibers and a rapid diffusion in the energy storage materials to facilitate ion transport, (2) it is possible to devise dual ion diffusion and electron transfer pathways by optimization of the conductive material coatings. Such developments were demonstrated in the case of paper/CNT/MnO_2/CNT, which offered superior supercapacitor performance.[100] Extra electrolyte uptake through the porous fibers while the paper fibers act as an electrolyte reservoir can again be optimized by a CNT coating, resulting in dual ion-diffusion and electron-transfer pathways being enabled in the electrode configuration of the paper electrode containing single cellulose fiber after CNT-dip-coating, followed by the electrodeposition of MnO_2 and another CNT-dip-coating (Fig. 12(a)), which offers high capacitance and impressive rate capacity. More interesting is that there are extra ion-diffusion pathways due to the presence of open-pore channels extending along the fibers (Fig. 12(b) and (c)).

A conductive interwoven network capable of acting as a free-standing paper electrode can be constructed by distributing a graphene-nanosheet (GNS) coating on the cellulose fiber network, which is distributed through the macroporous networks due to the strong interactive sites to bind the GNSs (Fig. 13). This unique membrane overcomes the low strength and low porosity of graphene papers, while the cellulose fiber enhances ion transport through its pores, resulting in a good rate capability and long cycling stability with a high capacitance.[101] The homogeneous penetration of GNSs into the filter film (pores and fibers inside the GCP (graphene–cellulose paper)) and deposition in the voids between the fibers occurs. Among the few significant achievements made toward optimizing the electrical conductivity of the GCP–GNS system are: (1) flexibility in the graphene content selection by choosing filter papers with different porosities, (2) the maximum capacitance per geometric area can be achieved

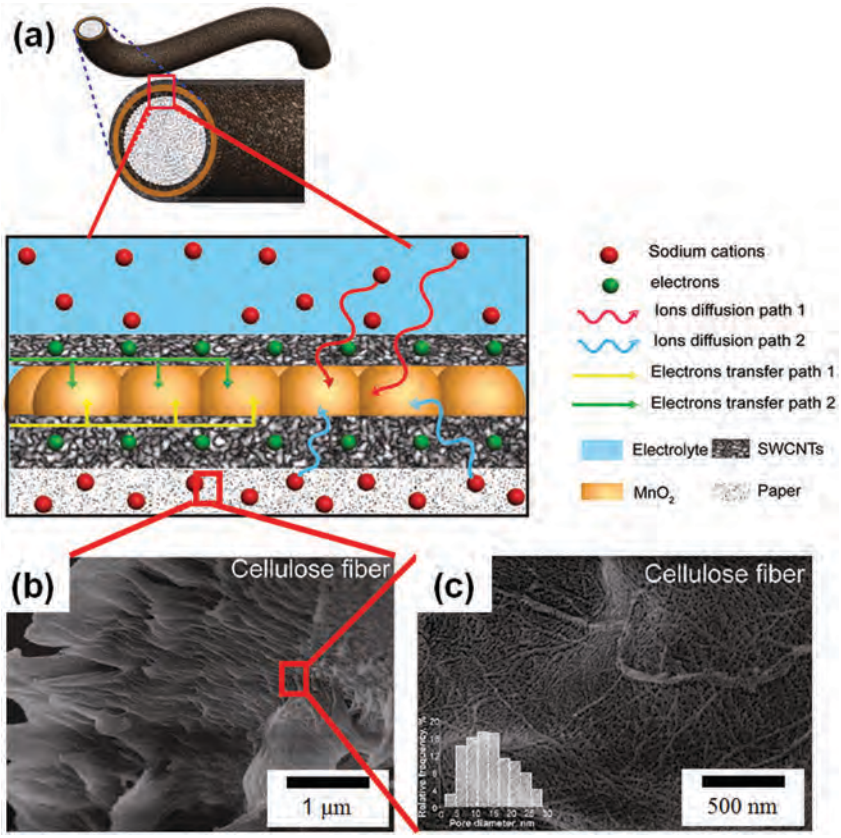

Fig. 12 (a) Schematic illustration of the highlighted area of one single cellulose fiber after CNT-dip-coating, followed by the electrodeposition of MnO_2 and a second CNT dip-coating. (b) and (c) SEM images of a magnified cross-section of a cellulose fiber and magnification of the surface of a cellulose fiber, respectively, after the fibers were sputtered with 2–5 nm gold to prevent localized charging and distortion, with the inset of (c) showing the pore size distribution (reproduced with permission from ref. 94, Copyright American Chemical Society, 2013).

with the highest GNS content (7.5%), (3) bending keeps the capacitance per geometric area at a high value, thus enabling versatile shaping of such conducting membranes. Good wettability of the cellulose fiber plays a major role in decreasing the charge-transfer resistance by favoring access of the ions into the GCP membrane. This implies a short ion-diffusion path for the GCP membrane as compared to the G-paper electrode, as revealed by electrochemical impedance spectroscopy (EIS). Such GCP membranes are good candidates for fabricating flexible polymer supercapacitors (poly-SCs) containing polymer–electrolyte, with the unique advantage of minimizing the device thickness.

In the case of cellulose paper (CP) electrodes with PPy coatings and flexible solid-state SCs based on PANI/Au/paper, the fabrication of CP-based asymmetrical thin-film SCs is a challenging goal. Thus, for enhancing the areal capacities and cycling performance, a multicomponent sandwich-structured graphite/Ni/Co_2NiO_4-CP was used as the positive electrode, which underpins the significance of the design and fabrication of flexible CP-based electrodes.[102] Generally, it is the surface roughness and insulation features of CP that create barriers for interconnections between materials (Fig. 13(a)). The most unique aspect of this multilayered cellulose-paper based electrode was the deposition of binary nickel–cobalt oxide, which offers greater electron conductivity and electrochemical activity, and therefore, also offers the potential for richer redox chemistry. Another key feature of such a multilayered cellulose-paper based electrode was the influence of the Ni layer on the electronic state of the Co_2NiO_4 layer, which ensures good capacitive performance and a high rate capability.

Instead of using a paper electrode, cellulose fibers extracted from waste paper can be used to form composites with graphene and PPy. The extraordinary features of free-standing binder-free electrodes composed of graphene–cellulose paper are well known; however, 3D interwoven structures of graphene–cellulose–PPy nanosheets offer excellent mechanical support along with high capacitance and good cycling stability.[103] It is essential to gain the synergistic effects of the different components of such cellulose-fiber based composite electrodes containing different layers of conductive materials with promising electronic or redox properties, as is illustrated by the above two cases of mixed metal oxide–graphene and PPy–graphene on cellulose-fiber electrodes. In the latter case, with the incorporation of porous cellulose fibers, potential drops in capacitance can be ameliorated. Thus, the low capacitive performance of PPy can be boosted by the use of porous cellulose fibers, apart from providing templates for the surface growth of the PPy and acting as a binder with enhanced mechanical stability. In the case of graphene or graphene–PPy, the incorporation of cellulose fibers causes the separated cellulose fibers to act as electrolyte reservoirs and this enhances electrolyte access for the coated graphene sheets, thus increasing the specific capacitance of the electrode.

In this process, the BC membrane has great potential as a perfect substrate for flexible supercapacitors. Free-standing, flexible, lightweight paper electrodes based on PANI-coated

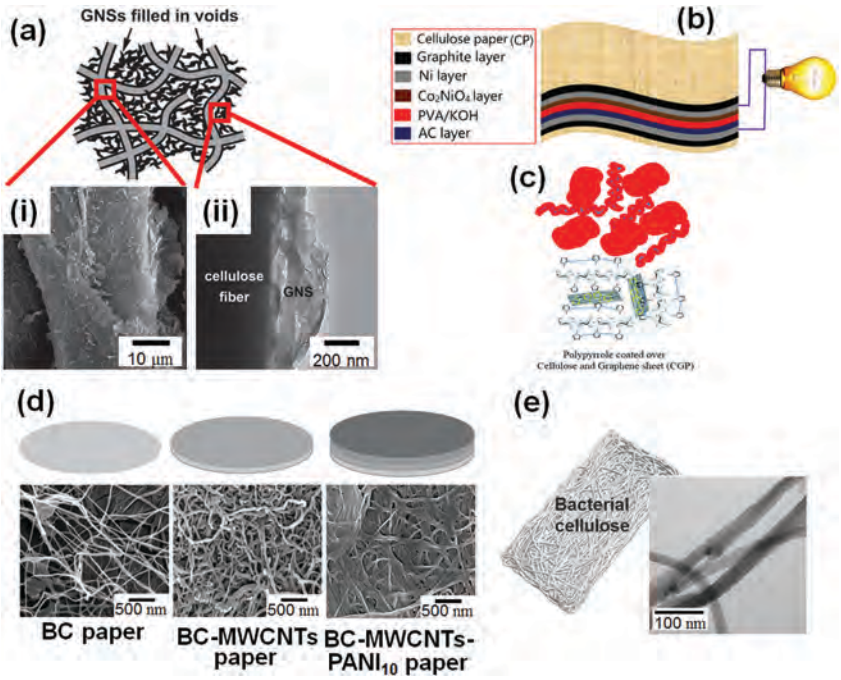

Fig. 13 (a) GNSs filling in the voids to construct a GCP electrode; (i) SEM and (ii) TEM images of a cellulose fiber in a GCP membrane, showing the GNSs anchored on the fiber surface (reproduced with permission from ref. 101, Copyright Wiley-VCH, 2011), (b) Schematic illustration of the assembled graphite/Ni/Co_2NiO_4-CP//graphite/Ni/activated carbon (AC)-CP asymmetrical thin film supercapacitors (ATFSCs), (c) polymer coated over cellulose and graphene sheet (CGP), (d) BC-paper electrode and its composite with MWCNT and MWCNT–PANI, typical energy filter TEM (EFTEM) image of N,PCNF electrode obtained from B, (e) Parent bacterial cellulose and energy filter TEM (EFTEM) of N- and P-doped CNF derived from BC (reproduced from ref. 105, Copyright Wiley-VCH, 2014).

BC for supercapacitors, fabricated with BC as the flexible substrate and MWCNT–PANI thin film as the current collector, result in a flexible supercapacitor.[104] The surface morphology and porous network among the BC nanofibers can be clearly identified (Fig. 13(a)), while in the BC–MWCNT paper (Fig. 13(b)), in which the MWCNTs are firmly connected with each other, they form a uniform 3D conducting nanoporous network on the BC paper, in which the pores of the MWCNT film are filled with PANI (Fig. 13(c)). The major advantages of the all-solid-state BC-based supercapacitor are: (1) high mechanical flexibility due to the flexible BC, and (2) strong mechanical bonding between the BC and MWCNTs. Thus, for flexible electronics, the feasibility of the flexible energy storage components of an electrode under various bending angles (00, 450, 900) means that the system exhibits stable cyclic voltammetry behavior at different bending angles, with its recoverable features confirmed.

BC has a huge potential for use in future materials when it is used for the fabrication of 3D carbon nanofibers with a promising degree of heteroatom (N, P, B) incorporation during pyrolysis. This general strategy of heteroatom doping into BC-derived nanofibers produces N,P-co-doped carbon nanofibers, which offer supercapacitors with high power density and excellent cycling stability,[105] 3D macroscopic heteroatom-doped carbon materials obtained from BC contain a unique 3D nanofiber network architecture, which enables ion transport along the 3D directions within the heteroatom-doped frameworks (Fig. 13(d)). Abundant functional groups on BC (Fig. 13(e)) allow for easy doping with the heteroatoms, which makes it possible for these functional carbon fibers Fig. 13(e) to enhance the power density of supercapacitors.[105]

Cotton-derived cellulose nanowhiskers, when used as carbon precursors and also as a hard template, can be used to obtain carbon *via* silica shell-entrapped cellulose nanowhiskers and with Co(II) ions to obtain carbon nanomaterials with metal oxide nanoparticles.[106] This material exhibits supercapacitive activity with double-layer capacitance. The excellent electrochemical properties of this material enable extending its scope for more electrochemical properties, which might largely depend on the Co_3O_4 content for the metal oxide/carbon nanomaterials with similar or better electrochemical properties. Similarly, graphenic nanofibers are accessible *via* a cellulose-derived and layer-by-layer stacked carbon fiber network electrode that exhibits uniform conductivity and an electro-adsorption/desorption phenomenon.[107] Graphenic carbon fiber also offers resistance from bacterial adhesion and proliferation, which is attributed to the layer-by-layer assembly of the hybrid electrode for the movement of ions on the carbon fiber network.

3D biotemplating is another emerging technique that has been witnessed using a carbonized BC-derived nitrogen-doped carbon nanofibers network, which essentially acts as facile template for decorating ultrathin nickel–cobalt-layered double hydroxide nanosheets for asymmetric supercapacitive applications.[108] Thus, polyaniline-coated BC nanofiber offers the N-doped carbon nanofiber for the further coating of metal hydroxides, where this hybrid electrode offers a high energy density at a low power density, reflecting the promises of a biomass-derived electrode for electrochemical energy storage. When compared with the BC-derived composite electrode with uniform layer-by-layer hydroxides and graphenic fibers, it is always the uniform distribution of double hydroxide nanosheets on the N-doped carbon that enhance the contact area between the electrode materials and electrolyte.

We can list several key features of CNF that have made CNF-based paper electrodes tremendously successful in many ways: (1) the greatly improved microstructures and electrical conductivity in flexible electrodes; (2) co-doping with heteroatoms is a far more fruitful strategy than using conductive additives and polymer binders that block the pores and increase the contact resistance; (3) the practical modification of the stiffness of CNF nanopaper and ability to use it as a reinforcing agent with a soft, ion-conducting polymer matrix. Not to detract from these developments, but to extend them further, it would be useful to study nature's hierarchical architectures as electrodes to capture their unique mechanical properties, which would represent another milestone in developing cellulose-fiber-based electrochemical devices.

Among the numerous cellulose-fiber-based composite electrodes, analysis of their supercapacitive potential offered an insight into the performances of these composite electrodes and allowed a comparison to be made with a number of conventional electrodes (Table 3). For example, the flexible GCP membrane electrode has a capacitance per geometric area of 81 mF cm^{-2}, which is equivalent to the gravimetric capacitance of 120 F g^{-1} of graphene.[101] Along with good capacitance, flexibility of the GCP thin-film is an added advantage for using it as a supercapacitor component as compared to conventional activated carbon electrodes.[109] The CNT-integrated cellulose composite with a room-temperature ionic liquid (CNT–cellulose–RTIL) offers a specific capacitance of 22 F g^{-1}, in which case, aqueous KOH electrolyte enhances the specific capacitance as compared to the non-aqueous RTIL.[97] The natural-fiber-based paper electrode (namely P-CMC) shows an improved rate performance with a higher initial specific capacitance. The dual electron pathways in the P-CMC sample result in a specific capacitance of 327 F g^{-1} at a scan rate of 10 mV s^{-1}, and this could be maintained at 201 F g^{-1} at 200 mV s^{-1} (61.5%). This performance essentially depends on the amount of CNT coated on the paper, which can be controlled by changing the dip-and-dry procedure repeat times.[100] Textile-based fibers offer a weaker capacitance as compared to cellulose-nanofiber-based composites of P-CMC. Carbon-nanoneedle-supported Co_3O_4 electrodes have been shown to have high supercapacitive charge storage properties as well as efficient catalytic activities toward the ORR. Specially, three different materials containing amorphous carbon nanoneedles were fabricated with relatively low (6.4%), moderate (57.5%), and high (81.4%) amounts of Co_3O_4, denoted as Co_3O_4/CNN-A, Co_3O_4/CNN-B, and Co_3O_4/CNN-C. Co_3O_4/CNN-A in particular afforded a high specific capacitance, which was attributed to its nanoneedle morphology, and most importantly, its high electrochemically active surface area.[106]

Owing to the porous structure and electrolyte absorption properties of BC paper, the flexible BC–MWCNT–PANI hybrid electrode offers an appreciable capacitance of 656 F g^{-1}.[104] This leads to remarkable cycling stability, with a minimum

Table 3 Comparison of the performance of cellulose-derived substrates as components (depositors as energy storage materials) of supercapacitor electrodes

Entry	Material	Structural features	Specific capacitance ($F\ g^{-1}$)	Power density ($kW\ kg^{-1}$)	Energy density ($W\ h\ kg^{-1}$)	Capacitance retention
1[100]	Cellulose paper/CNTs/MnO_2 (P-CM)	Mesoporous cellulose fiber with rough surface, interior electrolyte reservoir, ready diffusion of electrolyte into the energy storage material MnO_2	295 (10 mV s^{-1} scan rate) 96 (200 mV s^{-1})	283.63	32.91	95.4% capacity retention after 2000 cycles
2[100]	Cellulose paper/CNTs/MnO_2/CNT (P-CMC)	Mesoporous cellulose fiber with rough surface, interior electrolyte reservoir, with two CNT layers for two electron transfer path	327 (10 mV s^{-1} scan rate) 201 (200 mV s^{-1})	—	—	85% at 50 000th cycle
3[100]	Polyester textile/CNTs//CNT (T-CMC)	Smooth textile fiber with smooth surface, MnO_2 layer	—	—	—	62% at 12 500th cycle
4[97]	Nanocomposite paper (CNT cellulose-RTIL)	Cellulose plays the role of a spacer between the SWCNT electrodes, Ti/Au film deposited on exposed MWCNT acts a current collector. Film structure with large range of mechanical deformation	36	1.5	13	100 cycles
5[98]	PANI/Au/Paper electrode based on polyaniline fibers	PANI fiber with diameter of 100 nm tangled and twisted with each other, uniform and porous networks on Au-coated paper	560	3 ($W\ cm^{-3}$)	35	
6[99]	Graphene–polypyrrole composite film	Nucleation of polypyrrole polymer chains at the defect sites of the graphene surface	237	84	33	
7[102]	Graphite/Ni/Co_2NiO_4-CP (cellulose paper) (positive electrode) and graphite/Ni/AC-CP (negative electrode)	Cellulose paper asymmetric thin film with rough and porous CP with graphite and Ni coatings. Porous nanosheet consisting of sandwich structure of layers	1737	25.6	80	<4% capacitance loss after 20 000 cycles
8[105]	N,P-co-doped CNF	3D macroscopic with coadjacent nanofibrils and cross-linked pores with highly porous and ultrafine network of BC as the backbone	204	186	7.76	—
9[105]	B,N-co-doped CNF from BC	Coadjacent nanofibrils and cross-linked pores, intrinsic highly porous and ultrafine network of BC pellicles, carbon nanowires are interconnected with numerous junctions, unique 3D nanofiber network	204.9	0.201	3.8	Till 4000 cycles
10[104]	BC–MWCNTs–PANI	Porous structure with coating of MWCNTs	656	—	—	0.5% loss after 1000
11[101]	Graphene–cellulose paper (GCP)	Macroporous texture with high strength of cellulose filter paper, graphene nanosheets are strongly bound to the cellulose fibers, which results in graphene nanosheets covering the cellulose fibers and distributed through the macroporous texture of the filter paper to result in a conductive interwoven network	120	—	—	99% retained over 5000 cycles
12[106]	Co_3O_4/CNN Carbon nanoneedles supported Co_3O_4 electrode	Cellulose nanowhiskers used as carbon precursor and hard template for needle-shaped carbons	90.0	—	—	—

degradation of capacitance. When comparing the capacitance of cellulosic and non-cellulosic composites, PANI/Au/paper electrodes exhibit a capacitance of 350 $F\ g^{-1}$.[98] The fabricated graphite/Ni/AC-CP negative electrode also exhibits a large areal capacitance (180 mF) and features excellent cycling performances, with 98% C_{sp} retention after 15 000 cycles. Graphene/Ni/AC-CP exhibits a large areal capacitance of 180 mF cm^{-2}. Beside the great progress on graphene-hybrids with CP, a significant focus is currently directed toward the development of multilayered coatings on CP and the fabrication of CP-based asymmetrical thin films.

5. Other emerging areas

Robust cellulose nanocrystals (CNCs) with good biocompatibility, high crystallinity, and good mechanical tensile strength have been fostered in myriad areas, including enzyme immobilization, drug delivery, and biomedical applications.[110–112] Composites of CNCs with nanomaterials have led to structures with excellent hybrid support for enzymes. The current generation of materials scientists has striven to develop new processes to meet the demands for advanced materials, while also carrying out innovations in older ones with newer application profiles. Furthermore, there is a trend toward simpler approaches, to reduce both their price and environmental impact, including operations with a smaller number of units, thus boosting developments that lead to new applications. In this section, we outline some future perspectives from the literature on the emerging new applications of cellulose-based composites and analyze their future potentials.

5.1. Enzyme immobilization

As one example, a CNC/AuNPs matrix offers significant biocatalytic activity with excellent stability and recovery of specific activity for

enzymes.[99] A nanocomposite consisting of magnetite (Fe_3O_4) NPs and Au NPs was embedded on CNCs, which act as magnetic supports for the covalent conjugation of papain and also facilitate the recovery of immobilized papain, whereby an immobilized enzyme could retain 95% of its initial activity after a prolonged storage of 35 days at 4 °C.[113] We tried to correlate the surface composition and structure of CNC/Fe_3O_4NP/AuNP with the immobilization of enzyme activity. Fig. 14 describes the potential of magnetized CNCs as an efficient support matrix to serve as a superior immobilizing platform for enzymes, proteins and other biomaterials. Magnetic CNCs are well known to have many advantages,[114] and the conjugation of such magnetic CNCs with AuNPs enables the electrochemical and spectrophotometric detection of enzyme immobilization in addition to conventional enzyme assays.

5.2. Flexible electronics

Functional printing techniques are some of the most promising foundations of information technology.[115] Functional 3D arrays of carbon are one of the solutions for integrating printing techniques with high temperature processing, which is a key requirement for future electronics. In a recent study on the use of catalytic ink and paper support, cellulose was used to generate functional carbon/ceramic arrays with a 3D structure on a suitable large scale to enable the high temperature production of materials with applications as electrodes.[116] By filling the cartridge of an inkjet printer with a metal catalyst precursor and then printing, defined 2D lateral patterns were produced on clean cellulose paper, in which the resolution was controlled by the paper structure. Then, by providing shape processing or simple folding to a desired 3D structure, followed by the thermal conversion of this cellulose–paper composite, a conductive structure of iron–carbide in graphitic carbon could be produced. In Fig. 15(a), thin paper mounted on an A4 sheet of inkjet printer is shown. After printing with catalytic ink (iron precursor) (Fig. 15(b)) and calcination (Fig. 15(c)), the non-printed areas shrink slightly, which results in a 3D appearance as made of amorphous carbon. The novelty of the process consists in retaining the spatial conformation of a 3D paper object. It was found that the catalytic carbonization of thin tissue paper demonstrates the flexibility and durability of the final materials in terms of the ease of handling and possibility for multiple applications. Amazingly, repetition of this catalytic carbonization process using powdered cellulose proved to be a good model system, confirming that the fiber essentially acts as a structural template. The potential of converted paper electrodes based on cellulose nanofibers is not fully realized yet; however, they exhibit tremendous potential for application as electrodes in fuel cells and batteries, where co-printing with appropriate metal precursors can directly lead to access to functional devices.

5.3. Atomic modeling of cellulose microfibrils

The development of new techniques for revealing insights into the macromolecular architecture to extract the nanoscale geometry of cellulose microfibrils is an important fundamental strategy for the better design of materials and biomass treatments. Many current strategies for the catalytic deconstruction of biopolymers composed of lignocellulosic biomass employ thermochemical pretreatments to assist in penetration of the enzymatic and chemical catalysts into the cell walls. Current modeling approaches have offered valuable insights into the optimization of the biomass conversion process. This process can further be accelerated though by accurate models of the cellulosic macromolecular architecture by employing characterization and analysis techniques specialized for such nanofibrous structural investigations. Existing models of cellulosic nanostructures based on experimental techniques[117] are conceptually useful, but do not allow for the computational evaluation facilitated by the atomistic models. This is needed in order to construct a model that is capable of probing the structures of cellulosic plant cell walls with nanometer resolution, which would bridge the critical gaps in our understanding of cellulosic biomass with its complex polymer matrix architecture. Electron tomography is a part of advanced transmission electron microscopy (TEM), which captures 3D structure and bridges the gap between the atomic resolution obtained from X-ray crystallography and light microscopic imaging techniques.[118,119] Recent studies have demonstrated the applicability of electron tomography to investigate the 3D structures of cellulosic cell walls in biomass samples, in which user-driven segmentation and surface generation resulted in qualitative conclusions.[120,121] A recent study using electron tomography and employing algorithmic optimization for the longitudinal axis of plant microfibrils measured the

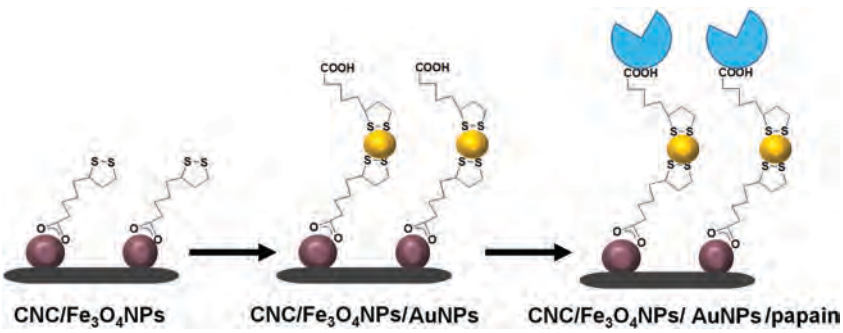

Fig. 14 Schematic illustration of the immobilization of enzymes on covalently functionalized CNC-functionalized Fe_3O_4NPs and AuNPs, which were later functionalized with papain enzyme to form the conjugate of CNC/Fe_3O_4NPs/AuNPs/Papain (drawn as shown in ref. 113, Copyright American Chemical Society, 2013).

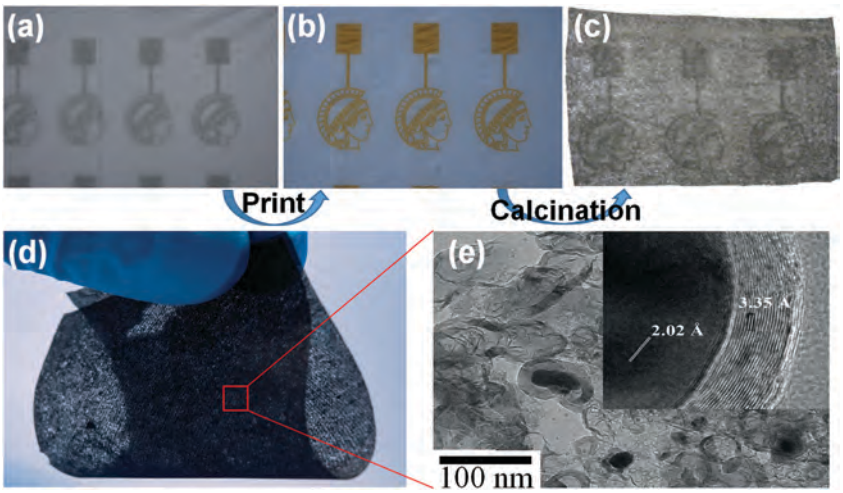

Fig. 15 (a) Thin paper with designs mounted on an A4 sheet of a regular inkjet printer, (b) the design after printing with catalytic ink, which included an iron precursor, (c) array of three printed Minervas after calcination, (d) photograph further illustrating the flexibility and transparency of the resulting paper electrode, (e) ultramicrotome TEM of a graphitized area and a high resolution micrograph with labeled lattice fringes (inset). (Images are reproduced from ref. 116 with permission, Copyright Wiley-VCH, 2013.)

curvature of microfibrils (Fig. 16(a)) using atomistic models for the first time. This allowed the construction of atomistic models of cellulose microfibrils with realistic nanoscale geometries, and it was found that the longitudinal curvature had an impact on the crystal orientation.[122] Kink formation was not observed in structures that were bent about the 100 plane (Fig. 16(b));

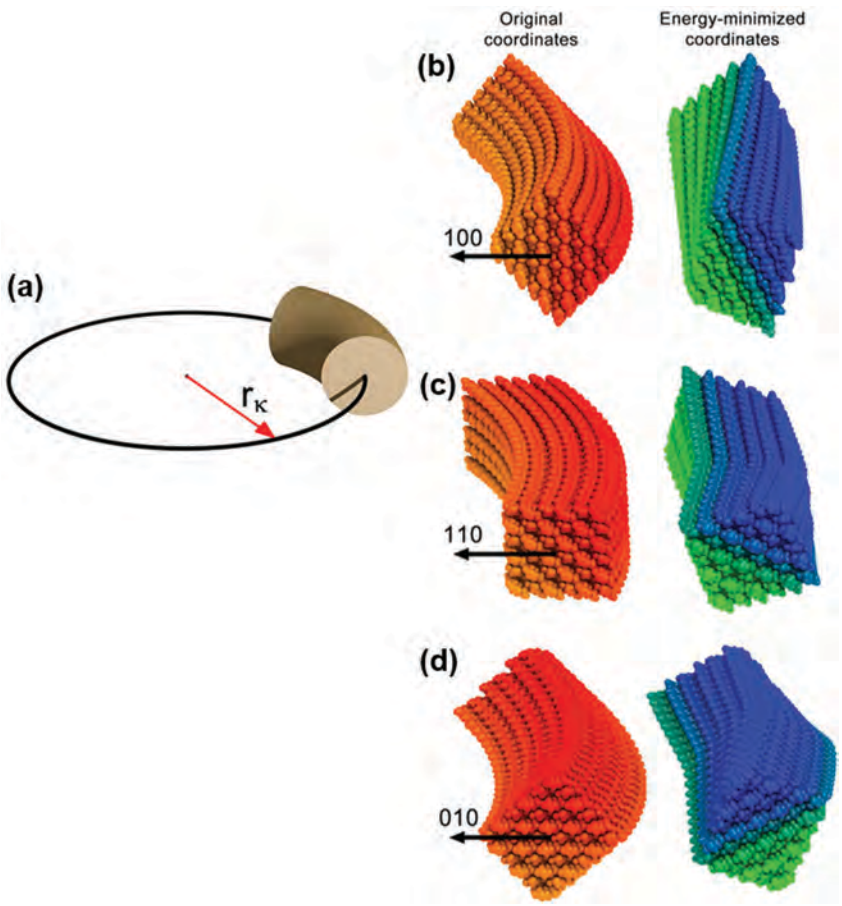

Fig. 16 Kink formation in atomistic models of cellulose microfibrils bent about the 100 and 010 crystal planes, exhibiting constant curvature (a). The coordinates were oriented such that the bending occurred about the 100 (b), 110 (c), and 010 (d) crystal planes (reproduced with permission from ref. 122, Copyright American Chemical Society, 2013).

however, energy minimization resulted in the formation of kinks in the models bent by magnitudes above a critical threshold about the 110 and 010 planes (Fig. 16(c) and (d)). This computational method was capable of analyzing microfibril structures of various bioresources and filamentous nanostructures. In addition, this method promises to be a relevant technique for industrially important feedstocks and thus has inherent utility for current cellulosic systems. The nanoscale geometry of cellulose microfibrils in pretreated biomass obtained from tomographic data sets shows that orienting the microfibrils model to bend about the 100 crystal plane reduces the formation of kink defects after energy minimization (Fig. 16). At this level of the atomistic model, a connection can be established between the directly observed nanoscale geometry and the proposed atomistic model, but this requires further improvement based on 3D nanoscale imaging, with quantitative image analysis necessary to conclusively segment and model the structures of cellulose and other forms of biopolymers.

6. Cellulose as a source of materials and its future impact

When carbon materials obtained from cellulose are employed in Na-ion supercapacitors, a significantly improved stable combination of energy and power can be achieved. The sodium ion capacitor requires the carbons to have different degrees of graphene ordering, surface area/porosity, and surface functionality for electrodes, so that such devices can be transformed into anodes and cathodes.[123] This is due to the highly heterogeneous structure, which consists of an interconnected cellulosic fibril network with individual microfibrils of 10–30 nm diameter, as revealed from the low magnification SEM image of PSNC-3-800 (Fig. 17(a)) (PSNC = peanut shell nanosheet carbon) and its higher magnification image revealing the carbon nanosheets (Fig. 17(b)). For adsorption cathode applications, cellulose microfibrils offer interconnected carbon nanosheets, which can be used as the adsorption cathode. Thickness analysis of PSNC-3-800 using high angle annular dark-field (HAADF) TEM, including low-loss electron energy loss spectroscopy (EELS) analysis, revealed the carbon nanostructure (Fig. 17(c)). The macroscopically open structure of PSOC-A (Fig. 17(d)) (PSOC = peanut shell ordered carbon) was obtained from the inner peanut shell, highlighting the typical sheet thickness to be in the order of 300 nm. Such a development of cellulose-nanostructure-based cathodes for energy storage would have a long-standing impact and widen the scope of utilizing cellulose microfibrils as an advanced materials source. Understanding some of the key factors that limit the performance of such cellulose-based supercapacitors is essential for further improvements.

The connection between the true 3D structures of cellulose microfibrils and the chemical processes occurring at the interface of the electrodes will inspire the fabrication of materials with 3D ordered structures. Conversion of the 3D network of cellulose into electrode materials can be compared with the inspiration behind the transfer of the structural design principals of biological materials to artificially made materials. It is thus considered that the extraordinary performance of the resulting materials from cellulose will play a major role in the future regarding the development of advanced functional devices made of cellulosic materials.

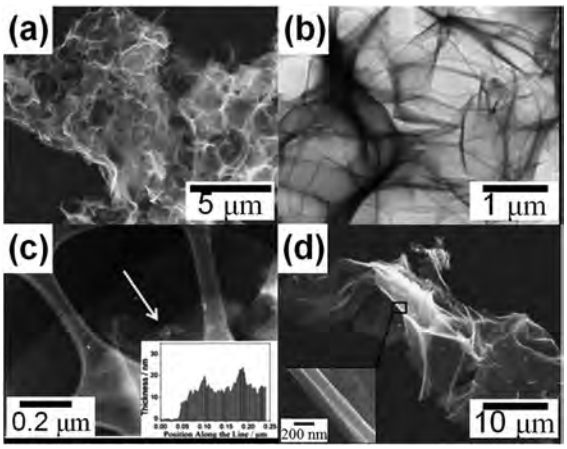

Fig. 17 (a) Low magnification SEM micrograph illustrating the macroscopic morphology of PSNC-3-800, (b) PSNC-3-800 at higher magnification, highlighting the morphology of the carbon nanosheets, (c) high angle annular dark-field (HAADF) image, with the inset showing a thickness profile of PSNC-3-800, measured with low-loss electron energy loss spectroscopy (EELS) along the white arrow, (d) low magnification SEM micrograph highlighting the morphology of PSOC-A, with the inset showing a magnified image highlighting the thickness of the carbon sheet (reproduced from ref. 123, Copyright, Royal Society of Chemistry, 2015).

7. Conclusions

New advanced electrochemical capacitors are emerging due to their superior power density, fast charge/discharge rates, and long cycle lifetime compared to other chemical energy storage devices. Further research is needed in order to improve their low energy density without sacrificing their power density and cycle life. Apart from developing asymmetric supercapacitors (ASCs) for improving the energy density,[124,125] much effort has been dedicated to exploring multicomponent hybrid electrode systems containing a porous carbon negative electrode and incorporating conducting materials as positive electrodes (*e.g.*, MnO_2). An advanced approach that has evolved recently is the incorporation of conductive nanomaterials into carbon electrodes, including carbon nanofoams, CNTs, and graphene.[126,127] This approach, however, suffers from the high cost of the CNTs and graphene for fabricating supercapacitors and other devices. Thus, the selection of carbon materials has driven a growing interest in the synthesis of carbon electrodes derived from biomass precursors, owing to their low cost, easy fabrication, environmental compatibility, and especially, the chances of exploring new nanostructures of biomass-derived electrodes.

In recent years, carbon-based materials have been made by a variety of natural ways and used for energy storage devices with enhanced electrochemical performance. In this regards, natural resources with a high proportion of cellulose are suitable for hierarchical pore networks. For example, carbon aerogels exhibit reasonable pore size distributions and supercapacitive energy

storage performances.[128] Functional aerogels containing N-doped graphene grafted onto cellulose fibers[129] and interconnected porous carbon frameworks with cellulose and graphene flakes[130] are some of the hybrid materials that have emerged for supercapacitive electrochemical applications.

Toward the further development of biomass-derived sources as electrodes, the emerging facts show the future directions: (1) fibrous materials can be directly converted to functional aerogels; (2) 3D framework fabrication can be achieved by using nanomaterials as composites; (3) to enable the development of miniaturized analytic platforms, bacterial nanopapers offer a diverse platform for optical(bio)sensing-based electronics. Exploring highly conducting CNFs and BC-derived functional materials has great potential for a range of applications, such as wearable electronics and low-cost energy storage, which should spur on efforts for the next-stage of developments.

Acknowledgements

S. D. acknowledges the pioneering work of all the researchers who have strengthened the development of the cellulose-based components of electrochemical devices and energy storage systems. This work was partially supported by the Australian Institute for Innovative Materials (AIIM) Gold/2017 grant. The author (K. W.) is grateful for the funding support from the Ministry of Science and Technology (MOST) of Taiwan (104-2628-E-002-008-MY3, 105-2911-I-002-560, 105-2221-E-002-227-MY3, and 105-2218-E-155-007) and National Taiwan University (105R7706).

References

1 D. D. Liana, B. Raguse, J. J. Gooding and E. Chow, *Sensors*, 2012, **12**, 11505–11526.
2 R. T. Olsson, M. A. S. Azizi Samir, G. Salazar Alvarez, L. Belova, V. Strom, L. A. Berglund, O. Ikkala, J. Nogues and U. W. Gedde, *Nat. Nanotechnol.*, 2010, **5**, 584–588.
3 R. Bendi and T. Imae, *RSC Adv.*, 2013, **3**, 16279–16282.
4 G. S. Armatas and M. G. Kanatzidis, *Science*, 2006, **313**, 817–820.
5 I. K. Moon, J. Lee, R. S. Ruoff and H. Lee, *Nat. Commun.*, 2010, **1**, 73–79.
6 *Annual Energy Outlook 2013 with Projections to 2040*, U.S. Energy Information Administration, Washington, DC, 2013.
7 P. Simon, Y. Gogotsi and B. Dunn, *Science*, 2014, **343**, 1210–1211.
8 J. Ren, L. Li, C. Chen, X. Chen, Z. Cai, L. Qiu, Y. Wang, X. Zhu and H. Peng, *Adv. Mater.*, 2013, **25**, 1155–1159.
9 H. Cheng, J. Liu, Y. Zhao, C. Hu, Z. Zhang, N. Chen, L. Jiang and L. Qu, *Angew. Chem., Int. Ed.*, 2013, **52**, 10482–10486.
10 T. Chen, S. Wang, Z. Yang, Q. Feng, X. Sun, L. Li, Z.-S. Wang and H. Peng, *Angew. Chem., Int. Ed.*, 2011, **50**, 1815–1819.
11 J. Zhang, Q. Kong, Z. Liu, S. Pang, L. Yue, J. Yao, X. Wang and G. Cui, *Solid State Ionics*, 2013, **245–246**, 49–55.
12 M. Kim, J.-Y. Shon, Y. C. Nho, T.-W. Lee and J. H. Park, *J. Electrochem. Soc.*, 2010, **157**, A31–A34.
13 P. Simon and Y. Gogotsi, *Acc. Chem. Res.*, 2013, **46**, 1094–1103.
14 Z. Chen, V. Augustyn, J. Wen, Y. Zhang, M. Shen, B. Dunn and Y. Lu, *Adv. Mater.*, 2011, **23**, 791–795.
15 H. Zhu, Z. Xiao, D. Liu, Y. Li, N. J. Weadock, Z. Fang, J. Huang and L. Hu, *Energy Environ. Sci.*, 2013, **6**, 2105–2111.
16 J. Huang, H. Zhu, Y. Chen, C. Preston, K. Rohrbach, J. Cumings and L. Hu, *ACS Nano*, 2013, **7**, 2106–2113.
17 W. Czaja, A. Krystynowicz, S. Bielecki and R. M. Brown Jr, *Biomaterials*, 2006, **27**, 145–151.
18 J. He, T. Kunitake and A. Nakao, *Chem. Mater.*, 2003, **15**, 4401–4406.
19 A. Dong, Y. Wang, Y. Tang, N. Ren, Y. Zhang, Y. Yue and Z. Gao, *Adv. Mater.*, 2002, **14**, 926–929.
20 D. Klemm, F. Kramer, S. Moritz, T. Lindström, M. Ankerfors, D. Gray and A. Dorris, *Angew. Chem., Int. Ed.*, 2011, **50**, 5438–5466.
21 R. J. Moon, A. Martini, J. Nairn, J. Simonsen and J. Youngblood, *Chem. Soc. Rev.*, 2011, **40**, 3941–3994.
22 L. Wang, C. Schutz, G. Salazar-Alvarez and M.-M. Titirici, *RSC Adv.*, 2014, **4**, 17549–17554.
23 X. Lu, P. J. Pellechia, J. R. V. Flora and N. D. Berge, *Bioresour. Technol.*, 2013, **138**, 180–190.
24 L. Wei, M. Sevilla, A. B. Fuertes, R. Mokaya and G. Yushin, *Adv. Energy Mater.*, 2011, **1**, 356–361.
25 O. Inganäs and S. Admassie, *Adv. Mater.*, 2014, **26**, 830–848.
26 H. Sun, L. Cao and L. Lu, *Energy Environ. Sci.*, 2012, **5**, 6206–6213.
27 M. Nogi and H. Yano, *Adv. Mater.*, 2008, **20**, 1849–1852.
28 G. Nyström, A. Mihranyan, A. Razaq, T. Lindström, L. Nyholm and M. Strømme, *J. Phys. Chem. B*, 2010, **114**, 4178–4182.
29 K. L. Spence, R. A. Venditti, O. J. Rojas, Y. Habibi and J. J. Pawlak, *Cellulose*, 2010, **17**, 835–848.
30 Z. Schnepp, *Angew. Chem., Int. Ed.*, 2013, **52**, 1096–1108.
31 H. Wang, E. Zhu, J. Yang, P. Zhou, D. Sun and W. Tang, *J. Phys. Chem. C*, 2012, **116**, 13013–13019.
32 Z.-Y. Wu, C. Li, H.-W. Liang, J.-F. Chen and S.-H. Yu, *Angew. Chem., Int. Ed.*, 2013, **52**, 2925–2929.
33 H. Yano, J. Sugiyama, A. N. Nakagaito, M. Nogi, T. Matsuura, M. Hikita and K. Handa, *Adv. Mater.*, 2005, **17**, 153–155.
34 M. M. Perez-Madrigal, M. G. Edo and C. Aleman, *Green Chem.*, 2016, **18**, 5930–5956.
35 R. A. Caruso, *Angew. Chem., Int. Ed.*, 2004, **43**, 2746–2748.
36 T. Serizawa, T. Sawada, H. Okura and M. Wada, *Biomacromolecules*, 2013, **14**, 613–617.
37 Q. Cheng, M. Li, L. Jiang and Z. Tang, *Adv. Mater.*, 2012, **24**, 1838–1843.
38 M. Pääkkö, M. Ankerfors, H. Kosonen, A. Nykänen, S. Ahola, M. Österberg, J. Ruokolainen, J. Laine, P. T. Larsson, O. Ikkala and T. Lindström, *Biomacromolecules*, 2007, **8**, 1934–1941.
39 J. Shi, Y. Hara, C. Sun, M. A. Anderson and X. Wang, *Nano Lett.*, 2011, **11**, 3413–3419.
40 M. Giese, L. K. Blusch, M. K. Khan, W. Y. Hamad and M. J. MacLachlan, *Angew. Chem., Int. Ed.*, 2014, **53**, 8880–8884.
41 J. A. Rogers, T. Someya and Y. Huang, *Science*, 2010, **327**, 1603–1607.
42 K. S. Kim, Y. Zhao, H. Jang, S. Y. Lee, J. M. Kim, K. S. Kim, J.-H. Ahn, P. Kim, J.-Y. Choi and B. H. Hong, *Nature*, 2009, **457**, 706–710.

43 S. Yamanaka and J. Sugiyama, *Cellulose*, 2000, **7**, 213–225.
44 L. Hu and Y. Cui, *Energy Environ. Sci.*, 2012, **5**, 6423–6435.
45 L. Hu, G. Zheng, J. Yao, N. Liu, B. Weil, M. Eskilsson, E. Karabulut, Z. Ruan, S. Fan, J. T. Bloking, M. D. McGehee, L. Wagberg and Y. Cui, *Energy Environ. Sci.*, 2013, **6**, 513–518.
46 K. Gao, Z. Shao, X. Wu, X. Wang, Y. Zhang, W. Wang and F. Wang, *Nanoscale*, 2013, **5**, 5307–5311.
47 B. Wang, X. Li, B. Luo, J. Yang, X. Wang, Q. Song, S. Chen and L. Zhi, *Small*, 2013, **9**, 2399–2404.
48 K. Yoshino, R. Matsuoka, K. Nogami, S. Yamanaka, K. Watanabe, M. Takahashi and M. Honma, *J. Appl. Phys.*, 1990, **68**, 1720–1725.
49 H.-W. Liang, Q.-F. Guan, Z. Zhu, L.-T. Song, H.-B. Yao, X. Lei and S.-H. Yu, *NPG Asia Mater.*, 2012, **4**, e19.
50 S. H. Yoon, H.-J. Jin, M.-C. Kook and Y. R. Pyun, *Biomacromolecules*, 2006, **7**, 1280–1284.
51 X. Wang, D. Kong, Y. Zhang, B. Wang, X. Li, T. Qiu, Q. Song, J. Ning, Y. Song and L. Zhi, *Nanoscale*, 2016, **8**, 9146–9150.
52 S. Virji, R. B. Kaner and B. H. Weiller, *J. Phys. Chem. B*, 2006, **110**, 22266–22270.
53 F. Rodríguez, M. M. Castillo-Ortega, J. C. Encinas, H. Grijalva, F. Brown, V. M. Sánchez-Corrales and V. M. Castaño, *J. Appl. Polym. Sci.*, 2009, **111**, 1216–1224.
54 J. Kim, S. Yun, S. K. Mahadeva, K. Yun, S. Y. Yang and M. Maniruzzaman, *Sensors*, 2010, **10**, 1473–1485.
55 O. van den Berg, M. Schroeter, J. R. Capadona and C. Weder, *J. Mater. Chem.*, 2007, **17**, 2746–2753.
56 A. A. Qaiser, M. M. Hyland and D. A. Patterson, *J. Phys. Chem. B*, 2011, **115**, 1652–1661.
57 L. H. C. Mattoso, E. S. Medeiros, D. A. Baker, J. Avloni, D. F. Wood and W. J. Orts, *J. Nanosci. Nanotechnol.*, 2009, **9**, 2917–2922.
58 A. Rußler, K. Sakakibara and T. Rosenau, *Cellulose*, 2011, **18**, 937–944.
59 H. S. O. Chan, P. K. H. Ho, S. C. Ng, B. T. G. Tan and K. L. Tan, *J. Am. Chem. Soc.*, 1995, **117**, 8517–8523.
60 W. Hu, S. Chen, Z. Yang, L. Liu and H. Wang, *J. Phys. Chem. B*, 2011, **115**, 8453–8457.
61 A. G. MacDiarmid, *Curr. Appl. Phys.*, 2001, **1**, 269–279.
62 S. Ameen, M. Shaheer Akhtar and M. Husain, *Sci. Adv. Mater.*, 2010, **2**, 441–462.
63 J. Huang and R. B. Kaner, *Chem. Commun.*, 2006, 367–376.
64 H. Wang, L. Bian, P. Zhou, J. Tang and W. Tang, *J. Mater. Chem. A*, 2013, **1**, 578–584.
65 D. Müller, C. R. Rambo, D. O. S. Recouvreux, L. M. Porto and G. M. O. Barra, *Synth. Met.*, 2011, **161**, 106–111.
66 T. K. Vishnuvardhan, V. R. Kulkarni, C. Basavaraja and S. C. Raghavendra, *Bull. Mater. Sci.*, 2006, **29**, 77–83.
67 H. Olsson, G. Nyström, M. Strømme, M. Sjödin and L. Nyholm, *Electrochem. Commun.*, 2011, **13**, 869–871.
68 K. F. Babu, R. Senthilkumar, M. Noel and M. A. Kulandainathan, *Synth. Met.*, 2009, **159**, 1353–1358.
69 D. Klemm, B. Heublein, H.-P. Fink and A. Bohn, *Angew. Chem., Int. Ed.*, 2005, **44**, 3358–3393.
70 Y. J. Kang, S.-J. Chun, S.-S. Lee, B.-Y. Kim, J. H. Kim, H. Chung, S.-Y. Lee and W. Kim, *ACS Nano*, 2012, **6**, 6400–6406.
71 F. Lai, Y.-E. Miao, L. Zuo, Y. Zhang and T. Liu, *ChemNanoMat*, 2016, **2**, 212–219.
72 X. Xu, J. Zhou, D. H. Nagaraju, L. Jiang, V. R. Marinov, G. Lubineau, H. N. Alshareef and M. Oh, *Adv. Funct. Mater.*, 2015, **25**, 3193–3202.
73 Q. Niu, K. Gao and Z. Shao, *Nanoscale*, 2014, **6**, 4083–4088.
74 L.-F. Chen, Z.-H. Huang, H.-W. Liang, Q.-F. Guan and S.-H. Yu, *Adv. Mater.*, 2013, **25**, 4746–4752.
75 Z. Lei, J. Zhang and X. S. Zhao, *J. Mater. Chem.*, 2012, **22**, 153–160.
76 H. Zhu, Z. Fang, Z. Wang, J. Dai, Y. Yao, F. Shen, C. Preston, W. Wu, P. Peng, N. Jang, Q. Yu, Z. Yu and L. Hu, *ACS Nano*, 2016, **10**, 1369–1377.
77 F. Shen, H. Zhu, W. Luo, J. Wan, L. Zhou, J. Dai, B. Zhao, X. Han, K. Fu and L. Hu, *ACS Appl. Mater. Interfaces*, 2015, **7**, 23291–23296.
78 L. Nyholm, G. Nyström, A. Mihranyan and M. Strømme, *Adv. Mater.*, 2011, **23**, 3751–3769.
79 M. Ebner, F. Marone, M. Stampanoni and V. Wood, *Science*, 2013, **342**, 716–720.
80 R. V. Noorden, *Nature*, 2014, **507**, 26–28.
81 X. Lu, J. R. V. Flora and N. D. Berge, *Bioresour. Technol.*, 2014, **154**, 229–239.
82 S. Leijonmarck, A. Cornell, G. Lindbergh and L. Wagberg, *J. Mater. Chem. A*, 2013, **1**, 4671–4677.
83 S.-J. Chun, E.-S. Choi, E.-H. Lee, J. H. Kim, S.-Y. Lee and S.-Y. Lee, *J. Mater. Chem.*, 2012, **22**, 16618–16626.
84 J. Zhang, Z. Liu, Q. Kong, C. Zhang, S. Pang, L. Yue, X. Wang, J. Yao and G. Cui, *ACS Appl. Mater. Interfaces*, 2013, **5**, 128–134.
85 J.-H. Kim, J.-H. Kim, E.-S. Choi, H. K. Yu, J. H. Kim, Q. Wu, S.-J. Chun, S.-Y. Lee and S.-Y. Lee, *J. Power Sources*, 2013, **242**, 533–540.
86 J. Zhang, L. Yue, Q. Kong, Z. Liu, X. Zhou, C. Zhang, Q. Xu, B. Zhang, G. Ding, B. Qin, Y. Duan, Q. Wang, J. Yao, G. Cui and L. Chen, *Sci. Rep.*, 2014, **4**, 3935.
87 J. Ding, Y. Kong, P. Li and J. Yang, *J. Electrochem. Soc.*, 2012, **159**, A1474–A1480.
88 A. Chiappone, J. R. Nair, C. Gerbaldi, L. Jabbour, R. Bongiovanni, E. Zeno, D. Beneventi and N. Penazzi, *J. Power Sources*, 2011, **196**, 10280–10288.
89 M. Willgert, S. Leijonmarck, G. Lindbergh, E. Malmstrom and M. Johansson, *J. Mater. Chem. A*, 2014, **2**, 13556–13564.
90 L. Jabbour, M. Destro, D. Chaussy, C. Gerbaldi, N. Penazzi, S. Bodoardo and D. Beneventi, *Cellulose*, 2013, **20**, 571–582.
91 S. Iwamoto, W. Kai, A. Isogai and T. Iwata, *Biomacromolecules*, 2009, **10**, 2571–2576.
92 S. Cao, X. Feng, Y. Song, X. Xue, H. Liu, M. Miao, J. Fang and L. Shi, *ACS Appl. Mater. Interfaces*, 2015, **7**, 10695–10701.
93 J. Chmiola, G. Yushin, Y. Gogotsi, C. Portet, P. Simon and P. L. Taberna, *Science*, 2006, **313**, 1760–1763.
94 Z. Niu, P. Luan, Q. Shao, H. Dong, J. Li, J. Chen, D. Zhao, L. Cai, W. Zhou, X. Chen and S. Xie, *Energy Environ. Sci.*, 2012, **5**, 8726–8733.

95 H.-P. Cong, X.-C. Ren, P. Wang and S.-H. Yu, *Energy Environ. Sci.*, 2013, **6**, 1185–1191.
96 A. Mihranyan, L. Nyholm, A. E. G. Bennett and M. Strømme, *J. Phys. Chem. B*, 2008, **112**, 12249–12255.
97 V. L. Pushparaj, M. M. Shaijumon, A. Kumar, S. Murugesan, L. Ci, R. Vajtai, R. J. Linhardt, O. Nalamasu and P. M. Ajayan, *Proc. Natl. Acad. Sci. U. S. A.*, 2007, **104**, 13574–13577.
98 L. Yuan, X. Xiao, T. Ding, J. Zhong, X. Zhang, Y. Shen, B. Hu, Y. Huang, J. Zhou and Z. L. Wang, *Angew. Chem., Int. Ed.*, 2012, **51**, 4934–4938.
99 A. Davies, P. Audette, B. Farrow, F. Hassan, Z. Chen, J.-Y. Choi and A. Yu, *J. Phys. Chem. C*, 2011, **115**, 17612–17620.
100 Z. Gui, H. Zhu, E. Gillette, X. Han, G. W. Rubloff, L. Hu and S. B. Lee, *ACS Nano*, 2013, **7**, 6037–6046.
101 Z. Weng, Y. Su, D.-W. Wang, F. Li, J. Du and H.-M. Cheng, *Adv. Energy Mater.*, 2011, **1**, 917–922.
102 J.-X. Feng, S.-H. Ye, A.-L. Wang, X.-F. Lu, Y.-X. Tong and G.-R. Li, *Adv. Funct. Mater.*, 2014, **24**, 7093–7101.
103 A. De Adhikari, R. Oraon, S. K. Tiwari, J. H. Lee and G. C. Nayak, *RSC Adv.*, 2015, **5**, 27347–27355.
104 S. Li, D. Huang, B. Zhang, X. Xu, M. Wang, G. Yang and Y. Shen, *Adv. Energy Mater.*, 2014, **4**, 1301655.
105 L.-F. Chen, Z.-H. Huang, H.-W. Liang, H.-L. Gao and S.-H. Yu, *Adv. Funct. Mater.*, 2014, **24**, 5104–5111.
106 R. Silva, G. M. Pereira, D. Voiry, M. Chhowalla and T. Asefa, *RSC Adv.*, 2015, **5**, 49385–49391.
107 N. Pugazhenthiran, S. Sen Gupta, A. Prabhath, M. Manikandan, J. R. Swathy, V. K. Raman and T. Pradeep, *ACS Appl. Mater. Interfaces*, 2015, **7**, 20156–20163.
108 F. Lai, Y.-E. Miao, L. Zuo, H. Lu, Y. Huang and T. Liu, *Small*, 2016, **12**, 3235–3244.
109 J. Gamby, P. L. Taberna, P. Simon, J. F. Fauvarque and M. Chesneau, *J. Power Sources*, 2001, **101**, 109–116.
110 K. A. Mahmoud, K. B. Male, S. Hrapovic and J. H. T. Luong, *ACS Appl. Mater. Interfaces*, 2009, **1**, 1383–1386.
111 S. Dong and M. Roman, *J. Am. Chem. Soc.*, 2007, **129**, 13810–13811.
112 K. A. Mahmoud, J. A. Mena, K. B. Male, S. Hrapovic, A. Kamen and J. H. T. Luong, *ACS Appl. Mater. Interfaces*, 2010, **2**, 2924–2932.
113 K. A. Mahmoud, E. Lam, S. Hrapovic and J. H. T. Luong, *ACS Appl. Mater. Interfaces*, 2013, **5**, 4978–4985.
114 R. H. Marchessault, G. Bremner and G. Chauve, *Polysaccharides for Drug Delivery and Pharmaceutical Applications*, American Chemical Society, 2006, ch. 1, vol. 934, pp. 3–17.
115 L. Venema, *Nature*, 2011, **479**, 309.
116 S. Glatzel, Z. Schnepp and C. Giordano, *Angew. Chem., Int. Ed.*, 2013, **52**, 2355–2358.
117 C. Somerville, S. Bauer, G. Brininstool, M. Facette, T. Hamann, J. Milne, E. Osborne, A. Paredez, S. Persson, T. Raab, S. Vorwerk and H. Youngs, *Science*, 2004, **306**, 2206–2211.
118 K. J. Batenburg, S. Bals, J. Sijbers, C. Kübel, P. A. Midgley, J. C. Hernandez, U. Kaiser, E. R. Encina, E. A. Coronado and G. Van Tendeloo, *Ultramicroscopy*, 2009, **109**, 730–740.
119 O. Ersen, C. Hirlimann, M. Drillon, J. Werckmann, F. Tihay, C. Pham-Huu, C. Crucifix and P. Schultz, *Solid State Sci.*, 2007, **9**, 1088–1098.
120 S. P. S. Chundawat, B. S. Donohoe, L. da Costa Sousa, T. Elder, U. P. Agarwal, F. Lu, J. Ralph, M. E. Himmel, V. Balan and B. E. Dale, *Energy Environ. Sci.*, 2011, **4**, 973–984.
121 B. S. Donohoe, S. R. Decker, M. P. Tucker, M. E. Himmel and T. B. Vinzant, *Biotechnol. Bioeng.*, 2008, **101**, 913–925.
122 P. N. Ciesielski, J. F. Matthews, M. P. Tucker, G. T. Beckham, M. F. Crowley, M. E. Himmel and B. S. Donohoe, *ACS Nano*, 2013, **7**, 8011–8019.
123 J. Ding, H. Wang, Z. Li, K. Cui, D. Karpuzov, X. Tan, A. Kohandehghan and D. Mitlin, *Energy Environ. Sci.*, 2015, **8**, 941–955.
124 Z.-S. Wu, W. Ren, D.-W. Wang, F. Li, B. Liu and H.-M. Cheng, *ACS Nano*, 2010, **4**, 5835–5842.
125 C. Long, T. Wei, J. Yan, L. Jiang and Z. Fan, *ACS Nano*, 2013, **7**, 11325–11332.
126 Z. Fan, J. Yan, T. Wei, L. Zhi, G. Ning, T. Li and F. Wei, *Adv. Funct. Mater.*, 2011, **21**, 2366–2375.
127 J. Yan, Z. Fan, T. Wei, W. Qian, M. Zhang and F. Wei, *Carbon*, 2010, **48**, 3825–3833.
128 P. Hao, Z. Zhao, J. Tian, H. Li, Y. Sang, G. Yu, H. Cai, H. Liu, C. P. Wong and A. Umar, *Nanoscale*, 2014, **6**, 12120–12129.
129 C. Wang, Y. Li, X. He, Y. Ding, Q. Peng, W. Zhao, E. Shi, S. Wu and A. Cao, *Nanoscale*, 2015, **7**, 7550–7558.
130 J. Huang, J. Wang, C. Wang, H. Zhang, C. Lu and J. Wang, *Chem. Mater.*, 2015, **27**, 2107–2113.